CUMENTATION PAGE

AD-A279 202

3. REPORT DATE	FINAL 15 Nov 90 TO 14 Feb 94

4. TITLE AND SUBTITLE

Industrial exploitation of an alternate technology for the production of HgCdTe epilayers, structures and devices

6. AUTHOR(S)

ARPA ORDER NO 7209

Professor Jean-Pierre Faurie

7. PERFORMING ORGANIZATION NAME(S) AND ADDRESS(ES)

EIPR, Ltd
P O Box 803827-P2E
Chicago IL 60680-3827

AFOSR-TR- 94 0281

9. SPONSORING/MONITORING AGENCY NAME(S) AND ADDRESS(ES)

AFOSR/NE
110 Duncan Avenue, Suite B115
Bolling AFB Washington DC 20332-0001

F49620-91-C-0007

11. SUPPLEMENTARY NOTES

12a. DISTRIBUTION/AVAILABILITY STATEMENT

APPROVED FOR PUBLIC RELEASE: DISTRIBUTION IS UNLIMITED

13. ABSTRACT (Maximum 200 words)

The program goals was: (1) Estimate the total cost to produce an MBE-grown HgCdTe epitaxial wafer suitable for the industrial manufacture of an IR photo diode detector array. (2) Establish manufacturing procedure for MBE-grown HgCdTe epitaxial layers in order to bring to the market a product which is suitable for FPAs. (3) Growth of high quality HgCdTe single epilayers and heterostructures with extremely uniform physical properties. The following characteristics, according to the program goals, were expected to be reached at the end of this program.

14. SUBJECT TERMS

17. SECURITY CLASSIFICATION OF REPORT	18. SECURITY CLASSIFICATION OF THIS PAGE	19. SECURITY CLASSIFICATION OF ABSTRACT	20. LIMITATION OF ABSTRACT
UNCLASSIFIED	UNCLASSIFIED	UNCLASSIFIED	UNLIMITED

NSN 7540-01-280-5500

EPIR LTD. EPITAXIAL INFRARED MATERIALS

INDUSTRIAL EXPLOITATION OF AN ALTERNATE TECHNOLOGY FOR THE PRODUCTION OF HgCdTe EPILAYERS, STRUCTURES AND DEVICES

DARPA CONTRACT MONITORED BY AFOSR

CONTRACT # F49620-91-C-0007

FINAL TECHNICAL REPORT

NOVEMBER 15, 1990 - FEBRUARY 14, 1994

JEAN-PIERRE FAURIE
PRINCIPAL INVESTIGATOR

P.O. BOX 803827-P2E, CHICAGO, IL 60680-3827 TELEPHONE: (312) 942-0841 FACSIMILE: (312) 942-1696

DARPA Contract # F49620-91-C-0007 entitled, "Industrial exploitation of an alternate technology for the production of HgCdTe epilayers" is monitored by the Air Force Office of Scientific Research (Lt. Col. G. Pomrenke).

PROGRAM GOALS

1. Estimate the total cost to produce an MBE-grown HgCdTe epitaxial wafer suitable for the industrial manufacture of an IR photo diode detector array.

2. Establish manufacturing procedure for MBE-grown HgCdTe epitaxial layers in order to bring to the market a product which is suitable for FPAs.

3. Growth of high quality HgCdTe single epilayers and heterostructures with extremely uniform physical properties. The following characteristics, according to the program goals, were expected to be reached at the end of this program:

I SINGLE EPILAYERS

$0.22 \leq x \leq 0.23$ with $\Delta x = \pm\ 2\times10^{-3}$ on 1x1cm^2

I-1	n-type layers:	N_d - N_a: (77K)	$\leq$	5×10^{15}cm^{-3}
		mobility: (77K)	$\geq$	1.0×10^5 cm$^2V^{-1}s^{-1}$
		lifetime: (77K)	$\geq$	0.5 μs
		EPD:	=	no specification
I-2	p-type layers:	N_a - N_d: (77K)	$\leq$	5×10^{15} cm^{-3}
		mobility: (77K)	$\geq$	300 cm$^2V^{-1}s^{-1}$
		lifetime: (77K)	$\geq$	10 ns at 77K
		EPD:	=	no specification

II HETEROSTRUCTURES

II-1* Planar Structure x=0.30, undoped, thickness 1-2μm on I-1 or I-2 epilayer - p-on-n in or n-on-p junction

II-2* Mesa Structure p-on-n in-situ doped heterostructure x=0.30, As-doped ($10^{17}cm^{-3}$ 1-2 μm on I-1 single epilayer

A total of 150 epilayers, homojunctions or heterojunctions were expected to be grown in this research program.

I CONTRACT ACHIEVEMENT SUMMARY

- **153** $Hg_{1-x}Cd_xTe$ single layers and heterostructures have been grown during this three year contract. They have been grown on (211)B CdZnTe substrates provided by various suppliers.
- The average $\overline{x}$ value for **122** epilayers is **0.2236** with a standard deviation σ of **1.28%** (σ=**0.59%** has been obtained for the last **20** epilayers grown exactly under the same growth conditions).
- The yield is equal to **0.80** for these 20 layers grown under the same conditions.
- Excellent composition and thickness uniformities have been obtained across a **2× 2** cm^2 wafer: $\sigma_x < \pm\ 5\times10^{-4}$ and **d/d< ± 0.0025**. The targeted σ_x value was $\perp\ 2\times10^{-3}$ for 1×1 cm^2. i.e much larger than what is achieved in MBE when the substrate is rotating.
- Excellent composition uniformity along the growth axis has also been achieved. A standard deviation σ_x **of** 5×10^{-4} which is within our measurement uncertainty has been found a for a 11μm thick layer with $\overline{x}$=0.220.
- Cost analysis has been performed confirming that MBE is cost competitive in HgCdTe growth technology.
- Analysis of the influence of the growth parameters on the quality of the epilayers has been performed and optimization has been realized.
  1. Under optimized growth conditions DCRC FWHM of HgCdTe epilayers duplicates that of CdZnTe(211)B substrate. **Best FWHM: 18 arcsec**
  2. MBE growth window is very narrow, the crystal quality deteriorates when the couple "Hg flux - growth temperature" is not precisely controlled (variation within 3C is allowed around the suitable optimization).
  3. MBE growth occurs under Te-rich conditions.
  4. Control of the doping through stoichiometry deviation is not possible.

5. MBE of HgCdTe seems to occur under condition close to equilibrium because mercury vacancy concentration Na is in relatively good agreement with the P-T phase diagram.

- A decrease in EPD is observed when FWHM is decreased; DCRC FWHM of 40 arcsec or less has been observed to be a necessary condition for EPD lower than 5×10^5 cm^{-2} Best EPD: 8×10^4 cm^{-2}.

- The main problem encountered during the 1st year was due to the diffusion of impurities (mostly acceptors) originating from the substrate. This problem has been observed for all the epilayers, however, the impurity level from supplier to supplier and even from lot to lot. NIMTEC substrates have been selected by EPIR Ltd.

- Indium has been used to control the residual doping. Excellent structural and electrical properties have been achieved. 2×10^{15} cm^{-3} is currently the lowest controllable n-type level. It has been found that this lower limit is still due to impurities diffusing from CdZnTe substrates.

- In-doped layers experienced p-type conversion through a suitable anneal. These Hg-vacancy doped p-type layers exhibit excellent characteristics.

- Minority Carrier lifetime of In-doped layers has been extensively studied. Lifetimes approaching 1 μs have been measured on low doped samples.

- Arsenic has been used to dope p-type through a new approach called delta doping. The results obtained are very promising. It has been found that As can be electrically activated at temperatures not exceeding 250C in 33% of the structures grown. This preserve tailored composition and /or doping profiles.

- Manufacturing procedures have been established.

At the end of this contract the layers produced at EPIR, on the basis of their structural and electrical properties are suitable for IR photodiode fabrication. The

characteristics of $Hg_{1-x}Cd_xTe$ (x=0.22) grown by MBE at EPIR are comparable if not better than those accepted in LPE technology on production lines (ref. 1).

II CONTRACT ACHIEVEMENTS

During the first year of this contract 50 undoped single epilayers have been grown on (211)B CdZnTe substrates. The main problem encountered during the 1st year was due to the diffusion of impurities (mostly acceptors) originating from the substrate. This problem has been observed for all the epilayers. However, the impurity level varied from supplier to supplier and even from lot to lot., After an extensive screening NIMTEC substrates have been selected by EPIR Ltd. The first year has been mostly devoted to optimize the growth conditions in order to obtain the highest crystalline quality for MBE grown layers.

The main goal during the second year of this program has been the control of extrinsic doping in MBE grown $Hg_{1-x}Cd_xTe$ epilayers. Indium has been used to control the n-type doping and $3\times10^{15}cm^{-3}$ was the lowest controllable level that has been achieved.

During the second and third year arsenic has been used to dope p-type through a new approach, i.e. delta doping. The results obtained are very promising since it has been found that As can be electrically activated at a temperature not exceeding 250C. However the control of the delta doping is not straightforward. We found that it requires a research effort by itself which was not the objective of this program. The third and final year of this contract has also been devoted to improve the structural and electrical properties of MBE-grown HgCdTe, to lower and understand the origin of the residual impurity background and to establish the basis for production of HgCdTe by MBE. A summary of the achievements obtained during this contract is presented hereafter.

Structural and electrical characteristics of the 153 $Hg_{1-x}Cd_xTe$ epilayers and heterostructures which have been grown during this 3 year project are reported in Table I to VII. Electrical data are reported only for doped layers and heterostructures grown during this program. The data related to undoped epilayers grown during the first year have been presented in the first report.

Table I - Unintentionally doped HgCdTe epilayers

Table II - Indium-doped HgCdTe epilayers

Table III - Electrical data of Indium-doped HgCdTe epilayers

Table IV - Arsenic Delta-doped HgCdTe epilayers

Table V - Electrical data of as-grown Arsenic Delta-doped HgCdTe epilayers

Table VI - Electrical data of annealed Arsenic Delta-doped HgCdTe epilayers

Table VII - Heterostructures

Table I
Unintentionally Doped HgCdTe Epilayers

Name	Substrate	x (%)	t (μm)	T_p (°C)	GR (°A/s)	Flux $\times 10^{-6}$	FWHM (arc.s)
007	CT-G	21.0	10.50	195	6.48	7.0	80
008	CT-5550-11-T	22.5	11.10	185	6.85	7.8	70
009	CT-5550-11A-T	23.8	08.60	195	4.33	9.0	65
010	CT-5550-12C-T	22.3	08.30	200	4.07	11.6	60
011	CT-5550-11D-T	23.3	10.30	190	4.76	8.5	100
012	CT-5607-10-T	22.0	09.60	190	4.71	6.0	38
013	CZT-5607-14-T	22.6	10.70	185	4.97	6.0	60
014	CZT-5498-19C-T	21.3	11.75	185	5.44	5.7	55
015	CZT-5498-6-T	20.5	10.92	185	5.69	5.7	65
016	CZT-5607-18-T	23.2	09.53	185	5.78	5.4	35
017	CZT-5607-17-T	23.0	10.46	185	6.05	5.4	25
018	CZT-5607-19-T	21.3	11.40	185	7.00	5.4	40
019	CZT-5498-6A-T	24.1	10.14	185	6.50	6.2	80
020	CZT-10139-11-TI	19.0	09.61	185	6.15	5.7	85
021	CZT-13009-10-TI	19.5	12.00	185	6.67	5.8	40
022	CZT-13018-9-TI	22.8	11.28	185	6.50	5.5	75
023	CZT-13000-8A-TI	24.8	09.85	185	6.84	5.7	65
024	CZT-13009-12-TI	18.0	11.43	185	7.10	5.7	65
025	CZT-5640-8-T	20.8	10.53	185	5.70	6.6	75
026	CZT-5640-9-T	24.0	13.90	185	5.90	7.2	165
027	CZT-5460-9-T	21.0	14.91	185	5.91	6.3	70
028	CZT-5460-10-T	20.1	14.00	185	6.14	6.0	80
029	CZT-5640-12-T	24.5	13.71	185	5.89	5.0	70
030	CZT-5640-12-T	24.0	11.00	175	5.73	4.5	70
031	CZT-5498-9-T	25.2	30.86	185	5.91	6.2	100
032	CZT-5498-9A-T	22.1	16.40	185	8.28	6.0	70
033	CZT-5498-17-T	22.1	15.67	185	10.45	6.0	185
034	CZT-5498-16A-T	22.0	12.30	188	9.76	5.1	70
035	CZT-5498-T	21.6	06.11	190	12.42	4.6	75
036	CZT-13009-10-T	23.3	09.00	184	7.01	6.0	105
037	CZT-5550-10D-T	22.0	15.56	175	3.96	3.4	-
038	CZT-1074-T	22.0	08.30	175	11.56	3.9	-
039	CZT-1075-T	20.0	15.79	185	14.50	3.6	105
040	CZT-5550-9C-T	21.3	23.80	189	13.63	3.3	105
041	CZT-B-0040-5-K	20.7	10.53	185	6.03	4.8	-
042	CZT-B-0040-4-K	21.0	10.00	195	5.63	5.8	70

Table I(continues)

Name	Substrate	x (%)	t (μm)	T_p (°C)	GR (°A/s)	Flux $\times 10^{-6}$	FWHM (arc.s)
043	CZT-B-0040-3-K	24.6	15.77	193	8.37	5.7	-
044	CZT-6991-N	24.2	08.30	185	3.20	5.5	100
045	CZT-6993-N	23.6	11.35	189	3.38	4.8	80
046	CZT-6994-N	23.1	15.20	189	4.69	5.4	70
047	CZT-6995-N	22.3	16.30	189	4.53	5.3	65
048	CZT-6996-N	23.1	16.90	189	4.65	5.0	53
049	CZT-6997-N	22.0	17.00	189	4.60	4.6	38
050	CZT-6998-N	21.3	09.80	189	4.88	3.8	40
051	CZT-7000-N	22.0	10.50	189	4.92	3.3	45
052	CZT-7001-N	22.9	10.90	189	4.71	2.8	61
053	CZT-7003-N	22.0	08.70	189	4.74	3.3	90
054	CZT-7002-N	20.4	15.80	189	4.67	4.2	65
055	CZT-13010-TI	20.9	08.60	189	4.52	4.1	40
056	CZT-B-0040-2-K	22.5	12.10	189	3.81	3.6	55
057	CZT-7004-N	22.7	10.70	189	3.84	5.1	68

Table II
Indium-Doped HgCdTe Epilayers

Name	Substrate	x (%)	t (μm)	T_p (°C)	GR (°A/s)	Flux $\times 10^{-6}$	FWHM (arc.s)	EPD $\times 10^{6}$
058	CZT-7514-N	21.0	10.60	-	-	-	52	02.44
059	CZT-7516-N	22.3	18.00	-	-	-	60	05.40
060	CZT-7515-N	21.8	10.40	-	-	-	22	01.86
061	CZT-7894-N	21.0	10.20	200	4.40	5.4	45	01.70
062	CZT-7893-N	22.1	12.90	202	3.90	5.0	33	20.17
063	CT-8143-N	21.8	14.59	202	3.40	5.4	38	01.14
064	CT-8141-N	23.4	14.59	201	3.00	5.1	45	06.33
065	CT-8142-N	22.6	10.81	202	3.30	5.2	47	06.42
066	CZT-7525-N	23.0	10.14	203	2.70	5.4	40	08.21
067	CT-7935-N	22.8	12.87	205	2.60	5.4	55	12.10
068	CZT-8279-N	22.6	09.30	202	3.60	5.4	36	00.92
069	CZT-8275-N	24.4	09.45	200	3.60	5.3	53	-
070	CZT-8276-N	20.5	14.20	202	3.94	5.5	35	01.86
071	CZT-8278-N	20.5	10.50	203	3.90	5.4	49	-
072	CZT-8281-N	23.7	11.54	201	5.10	5.6	48	00.18
073	CZT-8283-N	24.6	09.70	201	4.20	5.2	35	-
074	CZT-8080C-8-S	25.4	08.52	200	4.20	5.3	65	-
075	CZT-8530-N	22.0	10.30	212	4.80	5.4	51	00.18
076	CZT-8531-N	21.7	10.50	210	4.90	5.3	36	-
077	CZT-8532-N	22.2	11.40	210	5.30	5.5	42	00.13
078	CZT-8533-N	22.0	10.80	209	5.00	5.5	33	-
079	CZT-8534-N	22.7	11.12	212	5.20	5.3	50	-
080	CZT-8535-N	23.8	10.90	208	5.00	5.7	43	-
081	CZT-8536-N	22.4	10.30	207	4.80	5.6	45	-
082	CZT-8537-N	22.1	10.40	206	4.80	5.5	41	-
085	CZT-8080C-5-S	23.2	10.60	208	4.90	6.1	48	-
086	CZT-8080C-5-S	23.3	10.30	205	4.80	5.5	46	-
087	CZT-8080C-10-S	23.5	09.94	207	4.60	5.4	40	-
088	CZT-B0164-15K	23.3	11.90	205	5.50	5.7	62	26.10
089	CZT-J02733-1SB	21.6	10.30	200	4.80	5.5	43	12.60
090	CZT-733-2-SB	23.4	11.30	200	5.20	5.4	57	11.54
093	CZT-724-2-SB	23.3	10.80	200	5.00	5.4	55	07.96
094	CZT-735-2-SB	22.3	10.20	200	4.70	5.4	47	00.89

Table II(continues)

Name	Substrate	x (%)	t (μm)	T_p (°C)	GR (°A/s)	Flux $\times 10^{-6}$	FWHM (arc.s)	EPD $\times 10^{6}$
095	CZT-745-3-SB	23.4	11.00	200	4.70	5.6	18	-
098	CT-9032-N	23.5	09.40	203	4.60	4.8	36	-
099	CT-9031-N	23.1	19.90	202	4.30	5.2	-	-
100	CT-9033-N	22.0	16.40	204	4.40	4.7	-	-
109	CT-9042	-	24.60	185	-	-	-	-
110	CT-9043	-	15.40	185	-	-	-	-
111	CT-9044	22.0	12.20	185	-	-	-	-
112	CT-9045	19.4	10.00	185	-	-	-	-
113	CT-9046	22.6	12.10	185	-	-	-	-
114	CZT-9050	22.5	14.80	185	6.40	2.5	-	-
115	CZT-9049	23.7	18.80	185	-	2.6	-	-
121	CZT-9048	23.7	15.40	185	6.30	2.6	-	-
129	CZT-9109	30.1	09.70	190	-	-	-	-
130	CZT-9106	21.2	10.20	190	-	-	-	-
131	CZT-9400	21.4	09.40	191	5.20	3.6	-	-
132	CZT-9403	22.9	09.80	190	5.10	4.7	-	-
133	CZT-9399	22.9	10.60	190	5.30	4.6	-	-
134	CZT-9402	23.1	12.80	190	6.70	4.4	-	-
135	CZT-9384	23.3	09.50	190	17.00	5.0	-	-
136	CZT-9385	22.2	09.20	193	4.80	4.7	-	-
137	CZT-9401	22.0	09.60	190	4.80	5.0	-	-
145	CZT-9392	23.6	11.60	200	5.40	5.8	-	-

Table III **Electrical data of indium doped HgCdTe epilayers**

NAME	at 300K		at 80K		at 23K	
	C.C. (cm^{-3}) X10^{16}	Mob. (cm^2/Vs) x10^3	C.C. (cm^{-3}) X10^{15}	Mob. (cm^2/Vs) x10^4	C.C. (cm^{-3}) x10^{15}	Mob. (cm^2/Vs) x10^4
57	3.6	8.6	2.3	7.6	2.2	17.0
58	5.5	9.9	2.7	14.7	2.7	33.9
59	2.8	10.0	0.7	1.1	0.6	1.4(b)
60	5.8	9.1	1.9	9.8	1.3	1.6(b)
61	10.1	8.9	5.6	17.3	5.0	46.6
62	6.1	8.0	5.3	10.4	4.8	24.8
63	5.2	-	-	-	-	-
64	3.1	7.6	0.9	1.3	0.8	1.9(b)
65	4.9	5.8	3.7	4.3	3.5	6.8
66	5.0	6.2	10.5	4.4	9.6	9.1
67	4.3	8.1	8.5	5.3	8.0	9.8
68	4.8	7.8	23.1	6.0	22.0	10.5
69	3.8	7.1	21.2	5.8	20.4	10.5
70	7.9	10.7	25.4	13.0	24.6	16.9
71	6.9	9.2	21.4	8.7	20.9	13.2
72	3.8	7.5	4.4	7.6	4.3	15.5
73	2.3	6.0	3.8	5.7	3.7	10.0
74	2.3	4.3	1.5	1.9	1.2	2.7
75	4.1	7.1	2.3	9.5	2.1	23.2

76	5.0	6.3	3.1	8.1	2.7	19.5
77	3.6	7.1	2.0	7.6	1.8	15.6
78	3.9	7.4	2.4	9.6	2.42	22.9
79	3.4	6.8	2.6	5.2	2.4	8.9
80	2.2	5.5	2.1	3.7	1.4	5.4[b]
81	2.8	7.1	12.2	0.02(n)	1.4	0.03[b] (n)
82	3.1	8.7	1.3	9.5	1.2	20.2
85	2.8	6.8	2.8	4.1	2.7	8.3[b]
86	2.3	7.5	1.5	4.8	1.5	7.4[b]
87	-	-	-	-	-	-
88	-	-	-	-	-	-
89	3.4	7.4	3.8	5.0	2.1	0.8[b]
90	-	-	-	-	-	-
93	1.7	5.2	-	-	-	-
94	1.6	6.7	52.1 (p)	0.03(p)	20.3 (p)	0.03(p)
95	3.2	1.2	236.0 (p)	0.03 (p)	215.0 (p)	0.02(p)
98	3.1	6.7	4.8	4.5	4.5	7.3
99	4.4	5.4	3.8	2.3	3.6	3.4
100	3.4	8.2	1.5	7.0	1.5	13.6
109	2.3	6.3	9.2	5.5	8.8	10.2

110	4.1	7.6	5.4	10.0	5.2	21.1
111	4.8	8.8	5.6	10.5	5.5	21.9
112	6.0	8.3	7.9	9.7	7.6	22.6
113	3.2	7.6	5.5	7.1	5.4	14.0
114	-	-	-	-	-	-
115	-	-	-	-	-	-
121	-	-	-	-	-	-
129	3.4	6.5	10.0	0.4	9.5	0.4
130	5.6	3.3	47.0	1.5	45.0	2.3
131	4.4	5.3	18.0	0.3	15.0	0.3
132	2.2	7.2	3.6	1.1	3.2	1.5
133	-	-	-	-	-	-
134	2.6	6.8	5.1	0.7	4.8	0.9
135	2.7	8.2	0.5	3.5	0.4	9.8
136	3.4	7.3	7.2	1.2	7.7	1.8
137	4.5	6.3	4.1	3.1	3.9	0.5
145	3.0	7.2	2.5	2.3	2.4	3.7

(b) - Shows anomalous electrical data

Table IV
Arsenic Delta-Doped HgCdTe Epilayers

Name	Substrate	x (%)	t (μm)	T (°C)	Period (°A)	Flux $\times 10^{-6}$
091	CZT-164-13K	23.7	10.2	200	-	5.6
092	CZT-164-161K	22.5	10.6	200	-	5.5
096	CZT-745-5SB	50.0	02.0	205	-	5.0
097	CT-9034-N	39.0	08.2	210	-	5.2
101	CZT-5498-II-VI	24.2	04.5	-	96	-
102	CT-8145-N	25.3	02.5	-	-	-
103	CT-7939-N	19.8	12.0	-	-	-
104	CT-7941-N	19.9	17.0	-	-	-
105	CZT-5934-II-VI	-	08.0	-	-	-
106	CT-7938-N	38.0	19.3	198	193	-
107	CT-9041	27.7	10.0	195	-	7.1
108	CT-9039	27.2	08.0	175	-	4.4
116	CZT-9040	38.3	02.6	170	43	1.5
117	CZT-9113	32.9	04.6	175	42	1.5
118	CZT-9047	40.0	02.9	175	97	2.1
119	CZT-9111	41.9	02.9	175	97	1.5
120	CZT-9050	28.8	05.5	174	55	-
122	CZT-9112	46.5	05.4	185	54	1.7
123	CZT-9115	29.9	04.7	172	47	1.1
124	CZT-9114	31.7	04.5	185	136	2.1
125	CZT-9116	29.3	05.0	173	150	7.1
126	CZT-9118	26.1	05.0	174	50	1.4
127	CZT-9120	28.5	05.1	174	50	-
128	CZT-9121	32.1	02.5	191	33	1.2

Table V

Electrical Data (Mag. field B=0.8T) of as-grown Arsenic Delta-Doped HgCdTe Epilayers

Name	at 300K		at 80K		at 23K	
	C.C.(cm^{-3})	$\mu(cm^2/vs)$	C.C.(cm^{-3})	$\mu(cm^2/vs)$	C.C.(cm^{-3})	$\mu(cm^2/vs)$
091	2.1×10^{16}	7239	1.8×10^{14}	15718	8.5×10^{13}	45043
092	2.3×10^{16}	5690	5.2×10^{16}	195(p)	2.3×10^{16}	335(p)
096	7.0×10^{16}	36(p)	1.9×10^{16}	10(p)	-	-
097	-	-	-	-	-	-
101	2.4×10^{16}	3159	5.6×10^{16}	194(p)	4.0×10^{16}	175(p)
102	3.0×10^{16}	8034	4.2×10^{16}	84649	4.1×10^{15}	176803
103	7.2×10^{16}	8400	1.0×10^{16}	13300	5.4×10^{15}	7600
104	7.0×10^{16}	22900	1.1×10^{16}	46500	2.0×10^{15}	19200
105	9.7×10^{16}	16303	5.8×10^{15}	361206	5.0×10^{16}	150376
106	5.1×10^{14}	6667	2.2×10^{13}	114435	6.6×10^{13}	1298(p)
107	8.8×10^{15}	6502	9.1×10^{14}	29168	9.6×10^{14}	28516
108	1.2×10^{16}	4323	3.1×10^{15}	13483	3.2×10^{15}	17792
116	-	-	-	-	-	-
117	2.5×10^{15}	1757	9.8×10^{14}	536(p)	5.9×10^{14}	259(p)
118	4.2×10^{15}	17028	1.3×10^{15}	59912	1.6×10^{15}	54575
119	6.0×10^{14}	4900	1.2×10^{15}	9200(p)	-	-
120	8.0×10^{15}	6515	2.4×10^{15}	11386	2.4×10^{15}	15230
122	-	-	-	-	-	-
123	8.0×10^{15}	9062	5.5×10^{14}	87698	4.6×10^{15}	4455(p)
124	1.9×10^{16}	2366	4.0×10^{16}	478(n)	4.8×10^{16}	287(p)
125	7.4×10^{15}	6853	3.7×10^{15}	11691	3.6×10^{15}	10244
126	1.3×10^{16}	9227	8.8×10^{14}	62158	6.7×10^{14}	107898
127	8.9×10^{15}	10569	5.6×10^{14}	97880	3.7×10^{14}	35430
128	3.0×10^{15}	10304	208×10^{14}	165886	2.8×10^{114}	235352

Table VI
Electrical Data (Mag. field B=0.8T) of isothermal Annealed Arsenic Delta-Doped HgCdTe Epilayers

Name	at 300K		at 80K		at 23K	
	C.C.(cm^{-3})	μ(cm^2/vs)	C.C.(cm^{-3})	μ(cm^2/vs)	C.C.(cm^{-3})	μ(cm^2/vs)
091	2.1×10^{16}	7072	1.1×10^{15}	4676	6.9×10^{14}	6215
092	2.0×10^{16}	5223	6.1×10^{16}	284(p)	2.3×10^{16}	335(p)
096	1.2×10^{17}	45(p)	1.3×10^{16}	95(p)	-	-
097	7.0×10^{15}	2600	3.0×10^{14}	1500	2.0×10^{14}	3700
101	1.6×10^{16}	2080	1.2×10^{17}	266(p)	4.7×10^{16}	237(p)
102	3.1×10^{16}	4216	1.2×10^{16}	23959	1.2×10^{16}	38322
103	5.9×10^{17}	3200	5.6×10^{17}	5988	5.5×10^{17}	6884
104	4.2×10^{16}	11800	2.2×10^{15}	67800	2.4×10^{15}	1090
105	2.9×10^{17}	6711	2.4×10^{17}	20266	2.3×10^{17}	24498
106	6.1×10^{14}	1613	3.2×10^{15}	217(p)	3.4×10^{14}	165(p)
107	1.0×10^{16}	3322	6.7×10^{15}	5994	6.5×10^{15}	7624
108	4.4×10^{16}	1923	4.1×10^{16}	3849	4.0×10^{16}	4713
116	-	-	-	-	-	-
117	1.1×10^{16}	919	9.7×10^{15}	1473	-	-
118	4.1×10^{15}	2880	3.2×10^{15}	6867	-	-
119	9.0×10^{15}	873(n)	9.3×10^{15}	10(p)	-	-
120	5.2×10^{15}	3433	2.5×10^{15}	9801	2.3×10^{15}	13063
122	5.5×10^{15}	1168	3.7×10^{15}	3197	3.4×10^{15}	3298
123	2.3×10^{18}	11(p)	6.7×10^{16}	130(p)	1.6×10^{16}	100(p)
124	2.1×10^{16}	2828	1.9×10^{16}	9894	1.8×10^{16}	13216
125	3.4×10^{17}	1086	3.2×10^{17}	1807	3.2×10^{17}	1982
126	1.4×10^{17}	2425	1.2×10^{17}	5959	1.1×10^{17}	7277
127	2.5×10^{17}	2452	2.0×10^{17}	5510	1.9×10^{17}	6297
128	1.4×10^{16}	1235	1.4×10^{16}	2430	1.3×10^{16}	2000

Table VII
Heterostructures

Name	Substrate	x Base (%)	t (μm)	T (°C)	GR (°A/s)	Structure (Top/Bot.)	FWHM (arc.s)	EPD $\times 10^6$
083	CZT-8080C-11S	23.2	13.6	205	5.9	/In	37	2.17
084	CZT-8080C-12S	34.4	12.5	210	5.8	/In	35	2.13
138	CZT-9386	17.7	11.7	204	5.1	In/In	-	-
139	CZT-9387	22.7	11.2	201	5.8	In/In	97	0.31
140	CZT-9389	22.4	11.7	202	5.1	In/In	90	1.30
141	CZT-9390	22.4	11.4	204	5.0	In/In	90	0.17
142	CZT-9388	21.8	11.2	201	4.9	In/In	62	0.81
143	CZT-9391	22.7	11.3	201	5.0	In/In	45	0.71
144	CZT-9393	21.3	10.7	201	4.7	In/In	75	1.03
146	CZT-9881	22.4	10.9	190	5.3	As/In	25	0.40
147	CZT-9882	22.2	11.3	190	5.0	As/In	33	3.78
148	CZT-9887	22.3	13.3	186	5.9	As/In	-	-
149	CZT-9883	21.3	11.2	200	5.0	As/In	168	-
150	CZT-9884	21.9	11.4	200	5.0	As/In	19	-
151	CZT-9885	21.1	11.2	184	4.9	As/In	210	-
152	CZT-9888	21.8	11.7	185	5.1	As/In	33	-
153	CZT-9889	21.5	11.4	185	5.0	As/In	177	-
154	8087A#4	22.1	12.4	198	5.5	In/In	145	-
155	3035#2	22.1	11.3	195	5.0	In/In	103	-
156	8087A#2	22.9	11.8	195	5.2	In/In	105	-
157	8087A#7	21.9	11.0	190	4.8	In/In	50	-
158	8087A#8	21.0	11.3	192	5.0	In/In	170	-
159	8087A#13	23.0	11.7	191	5.2	In/In	228	-

III COMPOSITION AND YIELD ANALYSIS

Cost is obviously a very important criteria when selecting among technologies with similar capabilities. EPIR has estimated the cost on a previous DARPA contract entitled, "Evaluation of the feasibility and the cost of HgCdTe epitaxial layers grown by MBE on CdTe, CdZnTe, and GaAs substrate". EPIR has evaluated that the cost per cm^2 of HgCdTe grown on various substrates and in different MBE machine configuration ranges from $330 to $13 if the theoretical yield is 1.

The highest cost($330) is obtained for a 10 μm thick HgCdTe epilayer grown on a 3×3 cm^2 CdZnTe(211)B substrate in a MBE machine producing 200 epilayers per year. The lowest cost ($13) has been calculated for 5-inch HgCdTe epilayer grown on Si substrate in a MBE machine producing 400 to 600 epilayers per year. This cost even in the worst case, is far below $1,000, price which is currently paid for $1cm^2$ of LPE-HgCdTe grown on CdZnTe substrates.

One of the objectives of the current contract is to demonstrate that MBE can produce HgCdTe epilayers with an assigned composition of 0.22-0.23 and physical properties suitable for IR photodiodes as presented in the program goals. Run-to-run composition reproducibility, i.e. yield as well as composition uniformity were supposed to be established. The composition $\bar{x}$ averaged on 122 epilayers grown in this program falls within the target 0.220-0.230 with a standard deviation (σ) of 1.28% (Fig. 1). Standard deviation and yield have been improved since the installation of the new Te cell with a large capacity and keeps improving with growth parameter optimization. Standard deviation σ of 0.59% has been achieved on the last 20 epilayers grown during the third year. The yield has also improved since 80% of the last 20 layers grown in the program are acceptable in terms of composition (0.22 ± 0.002 - 0.23± 0.002) (see Fig 2).

In this yield analysis As-delta doped epilayers and a few other epilayers have not been considered since composition of 0.22-0.23 was not targeted. In addition it is important to point out that this program being a research and development program the optimization of the growth parameters very often induces a change in the targeted composition. A standard deviation of 0.59% is therefore actually better than expected. At EPIR we are convinced that a smaller standard deviation and a better yield can easily be achieved by MBE. Even with a yield of 0.80, the cost per cm^2

on a CdZnTe substrate will be in the worst case of 200 runs per year, at about $400 (330/0.80), i.e. less than half the selling price of LPE layers confirming that MBE is cost competitive in HgCdTe growth technology.

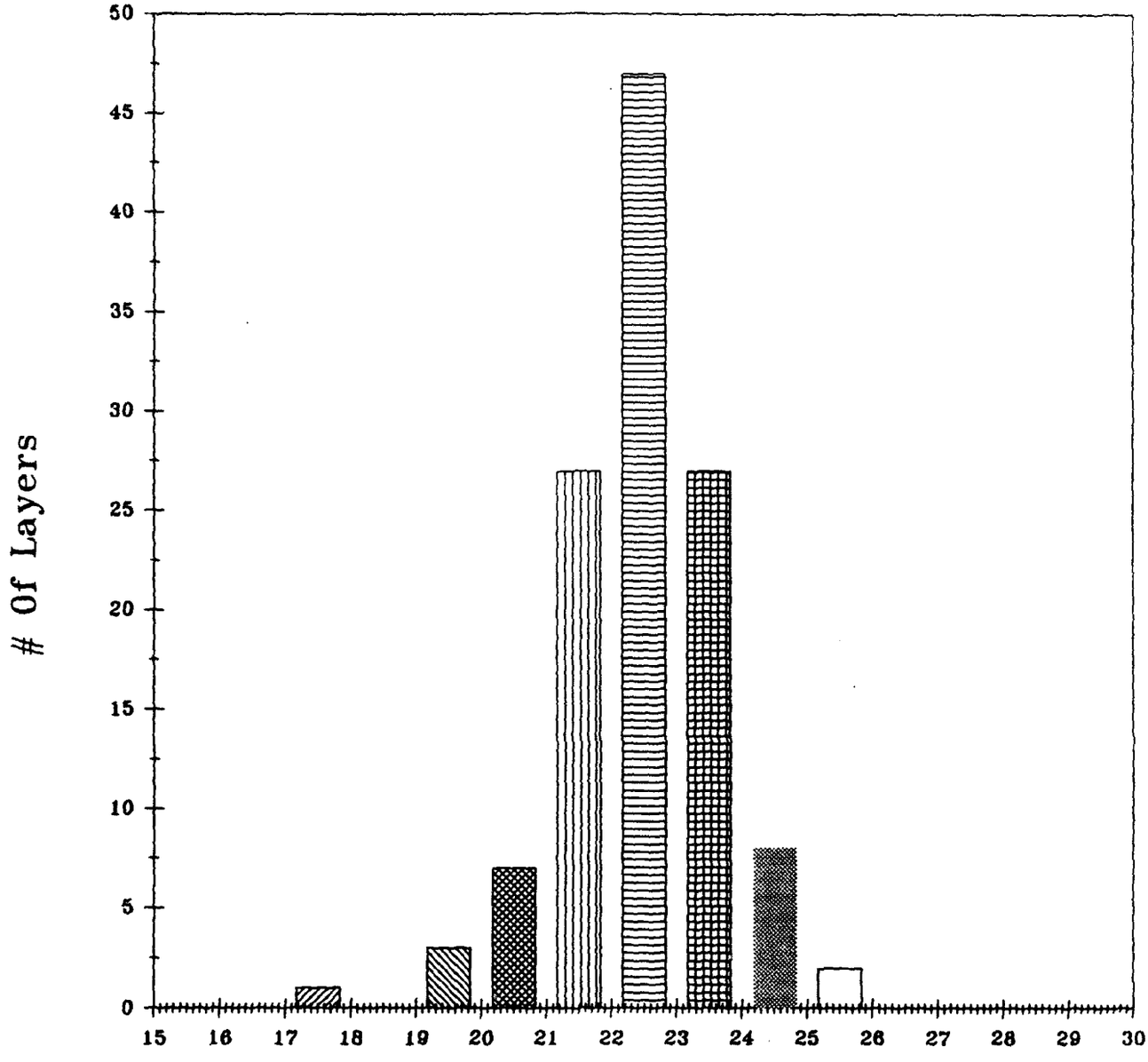

Mean x= 22.36%

Standard Deviation σ= 1.28

Total of 122 layers

Fig. 1

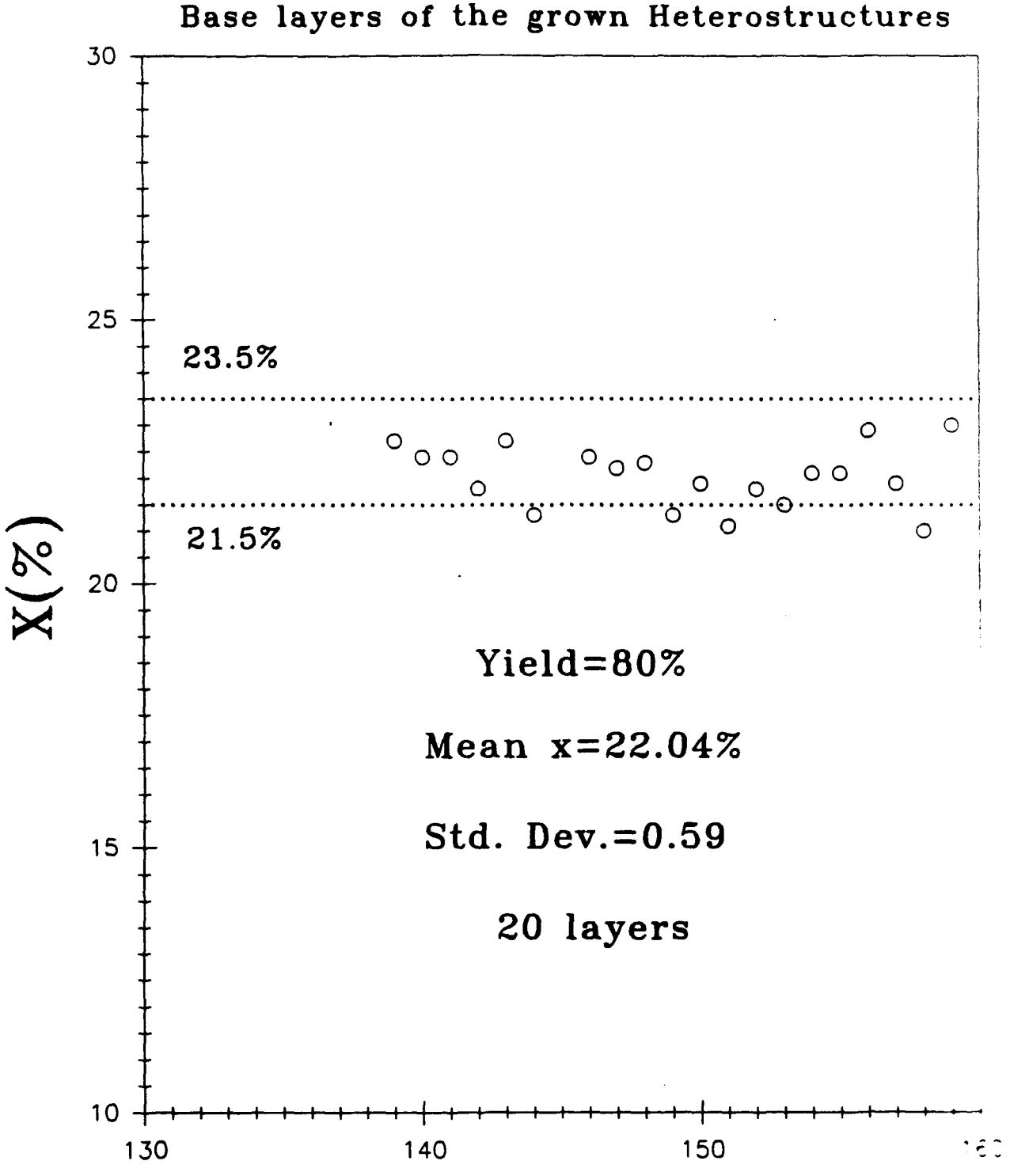
Base layers of the grown Heterostructures
30
25
20
15
10
X(%)
23.5%
21.5%
Yield=80%
Mean x=22.04%
Std. Dev.=0.59
20 layers
130
140
150
EPIR #

Fig. 2

IV COMPOSITION AND THICKNESS UNIFORMITY

During the first year EPIR has shown that uniformity in composition and thickness measured across 2×2 cm^2 wafer were within measurement uncertainty limits i.e.

$$\Delta x < \pm 5.0 \times 10^{-4}$$
$$\Delta x/x < \pm 2.2 \times 10^{-3}$$
$$\Delta d/d < \pm 2.5 \times 10^{-3}$$

These results obtained on a rotating substrate were much better than the goal assigned, *i.e.*Δx of $\pm 2 \times 10^{-3}$ on a 1×1 cm^2 substrate.

During the second year the composition uniformity along the growth axis, which to the best of our knowledge had never been previously measured for MBE layers, has been investigated. A profile of the absorption coefficient has been determined for sample #077 at different thicknesses through FTIR measurements. Figure 3a illustrates these measurements for three thicknesses : 3, 7.5 and 11 μm ; actually many other measurements have been performed. The spectra curves for energies above the bandgap were fitted to the following equation: $A(E\text{-}Ec)^b$. It can be seen that the intersection point Ec is almost the same along the growth axis Ec = 0.181 eV with a standard deviation σ=5×10^{-4} which is almost within the measurement uncertainty. Figure 3b displays the classical transmission curve of layer #077 as a signature of what FTIR spectra of 11 μm uniform HgCdTe epilayer should be.

This demonstrates that EPIR can grow MBE HgCdTe epilayers which do not exhibit measurable change in composition heither across 2×2 cm^2 wafer nor along the growth axis. Such a control in uniformity has never been demonstrated before by any growth technique. This reflects the knowledge of EPIR in controlling a substrate rotating during growth.

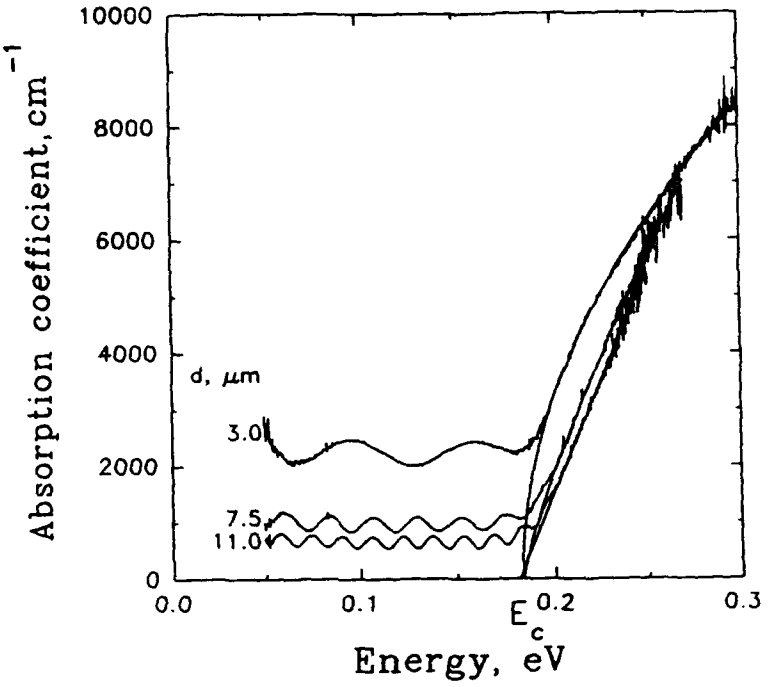
Absorption coefficient, cm^{-1}
10000
8000
6000
4000
2000
0
d, μm
3.0
7.5
11.0
0.0
0.1
0.2
0.3
E_c
Energy, eV

Fig. 3a

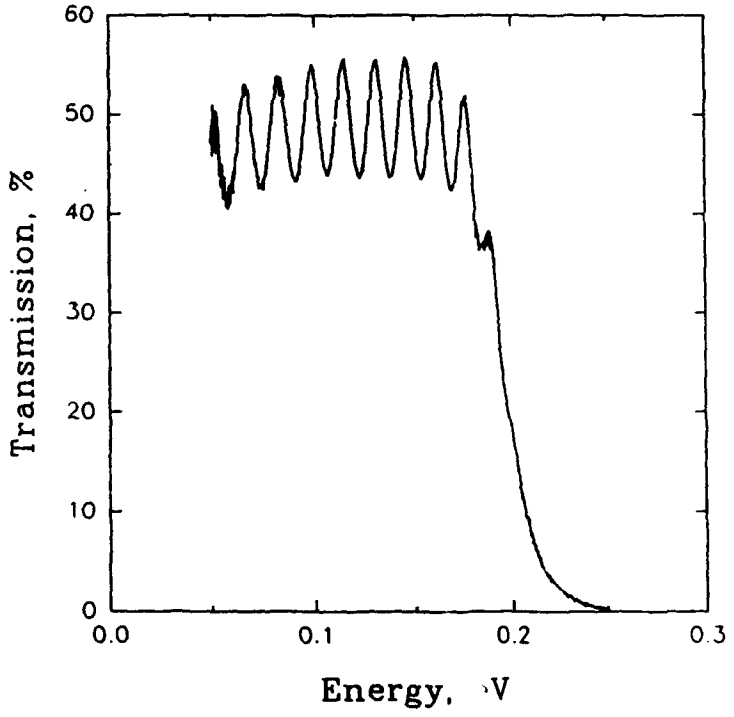
Transmission, %
60
50
40
30
20
10
0
0.0
0.1
0.2
0.3
Energy, eV

Fig. 3b

V ANALYSIS AND OPTIMIZATION OF THE GROWTH PARAMETERS

The growth of HgCdTe with a controlled and reproducible composition is obviously not enough to fulfill the requirement of suitability for IR photo diodes. Structural and electrical properties have to be investigated thoroughly before assessing the suitability of MBE-grown HgCdTe for IR manufacturing technology. This is what has been done in this program.

V-1 INFLUENCE OF THE GROWN CONDITIONS ON HgCdTe STRUCTURAL CHARACTERISTICS

During the first year a series of HgCdTe epilayers has been grown by MBE on (211)B CdZnTe substrate in order to analyze the influence of the growth parameters in view of their optimization. Double X-ray Rocking Curve (DCRC) FWHM has been the selected physical parameter since it provides very useful information about the crystal quality. DCRC FWHM is related to the dislocation density and to other as-grown defects present in the epilayer. The analysis has been carried out during the entire program and has produced very interesting results.

Figure 4 illustrates the change in DCRC FWHM vs Hg flux. In these experiments the growth temperature was 185C and the growth rate between 4 and 5 $\AA$/sec. The results confirm what has been previously observed, i.e. the crystal quality deteriorates when the Hg flux either is too low or too high. It is striking that the Hg flux "window" which allows the growth of the highest crystal quality is very narrow here, between 4 and 5.5 in arbitrary units. This represents a flux change of about 30% achieved by a change of only 3C in the Hg cell temperature. The same trend is observed when the growth rate increased but the window is even narrower, whereas the optimum Hg flux is about the same (Fig. 5 and 6). This information will have to be taken very seriously when the growth rate is increased. The good news is that under optimized growth conditions DCRC FWHM of MBE(211)B $Hg_{1-x}Cd_xTe$ duplicates that of (211)B CdZnTe substrates. The best result to date is 18 arcsec. DCRC FWHM of 20-30 arcsec should correspond to EPD's in the low 10^5 cm^{-2} range. This will be discussed in section V-2.

EPIR does confirm that MBE growth of HgCdTe requires a stringent control of the

growth parameters such as substrate temperature, Hg flux, and growth rate. However once understood MBE growth can be fully automated.

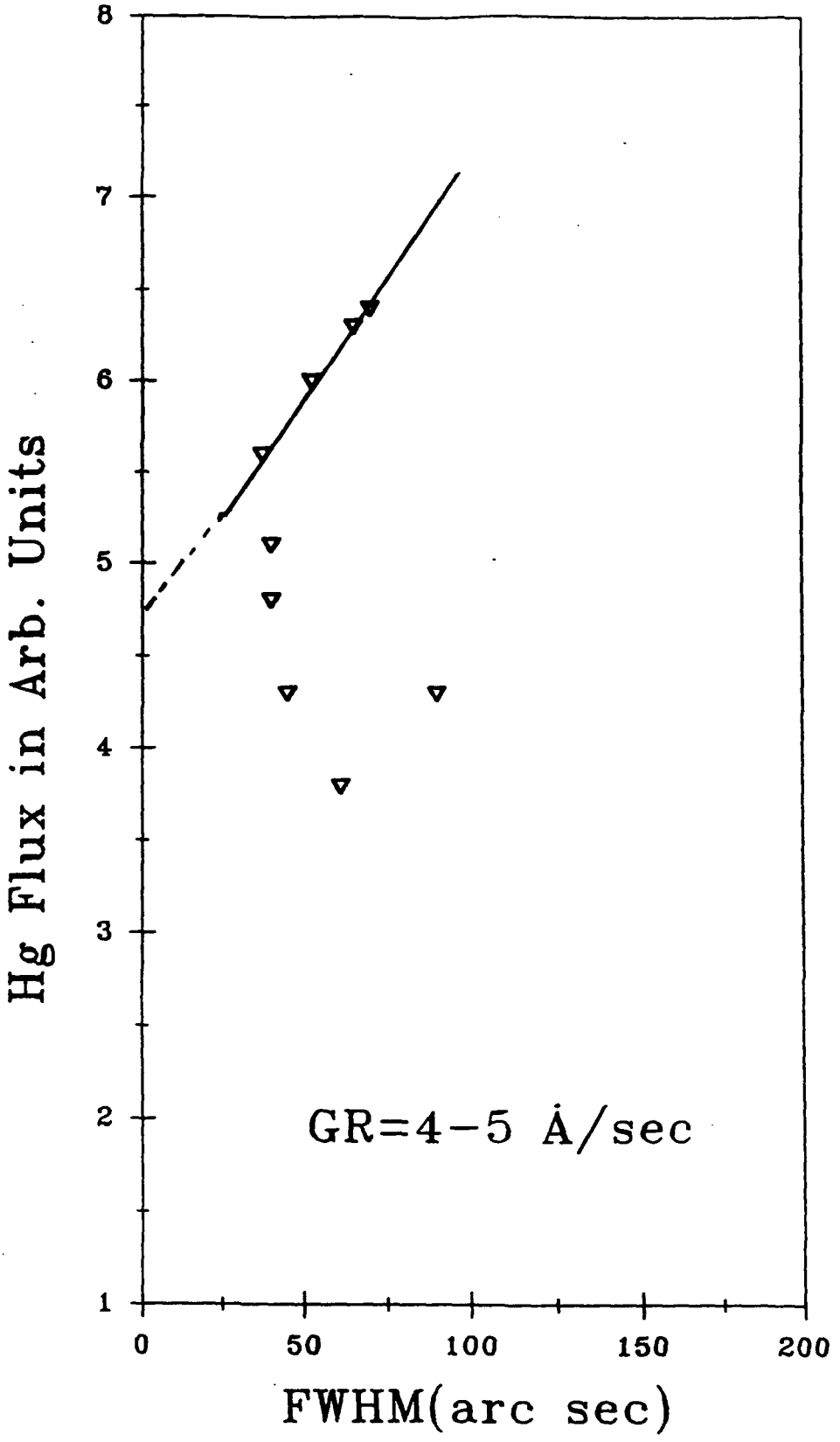
Hg Flux in Arb. Units
8
7
6
5
4
3
2
1
0
50
100
150
200
FWHM(arc sec)
GR=4-5 Å/sec

Fig. 4

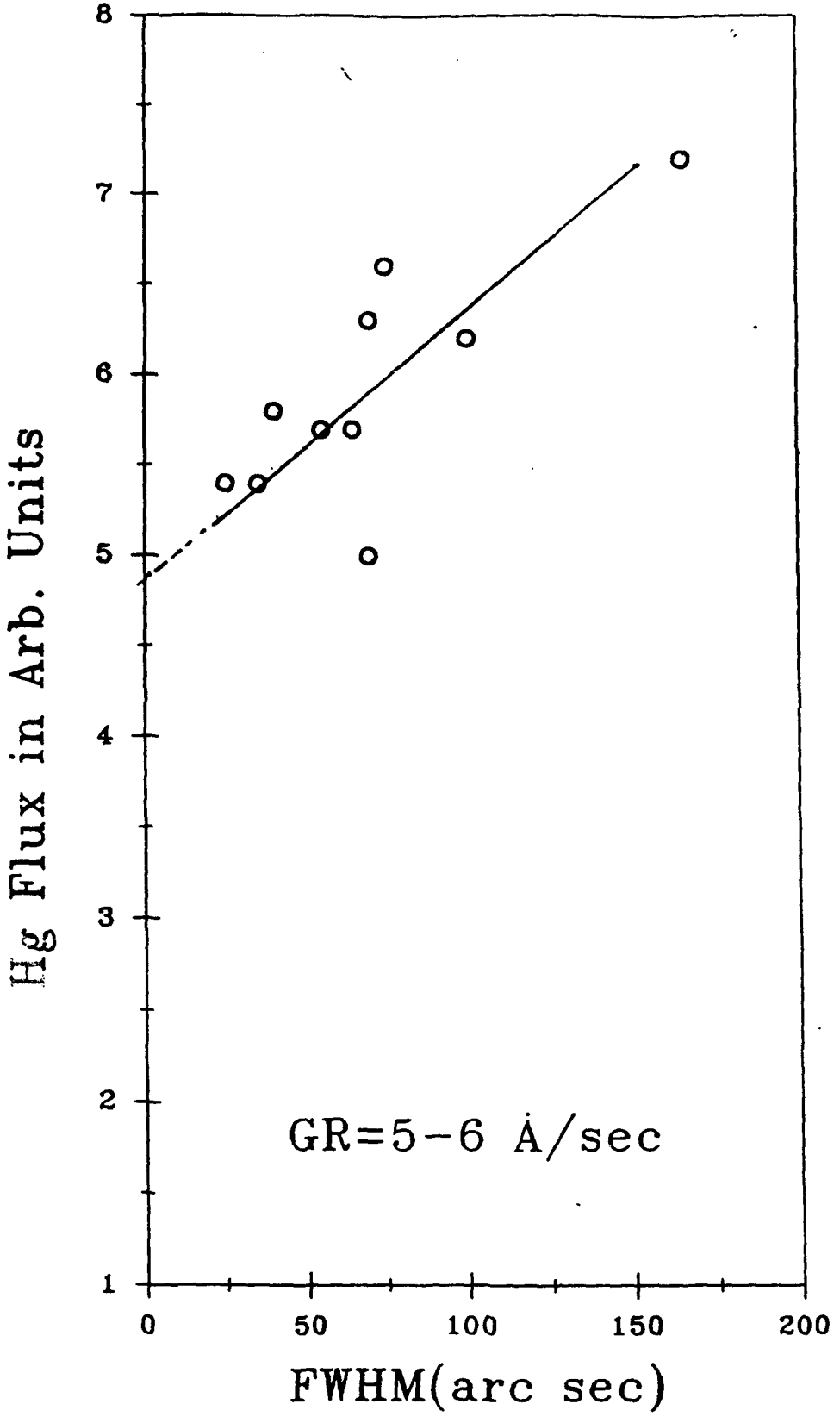
8
7
6
5
4
3
2
1
Hg Flux in Arb. Units
GR=5-6 Å/sec
0
50
100
150
200
FWHM(arc sec)

Fig. 5

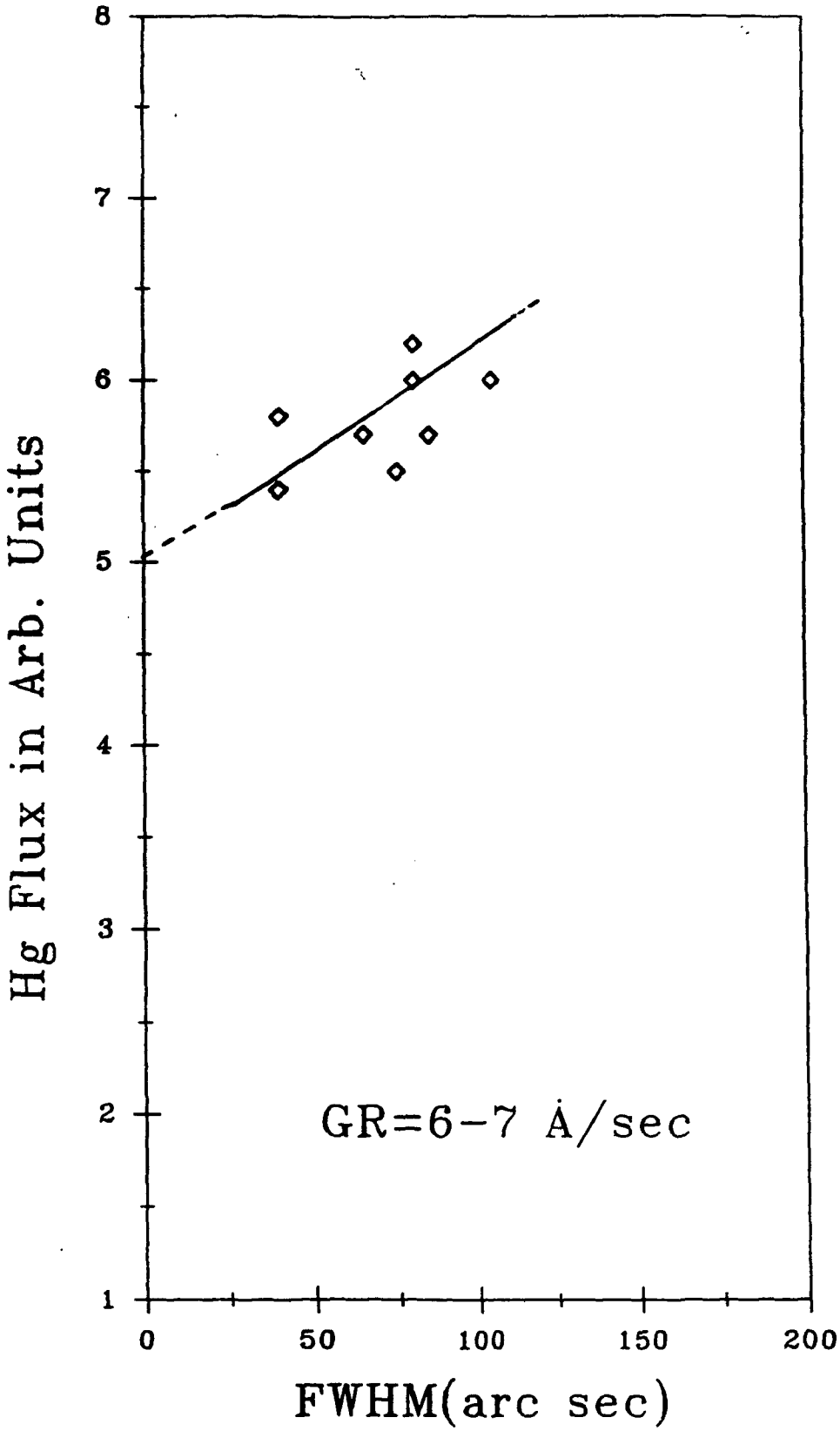
8
7
6
5
4
3
2
1
Hg Flux in Arb. Units
GR=6-7 Å/sec
0
50
100
150
200
FWHM(arc sec)

Fig. 6

V-2 DISLOCATION DENSITY MEASUREMENT

It is widely recognized that defects are limiting HgCdTe device performances and therefore FPA operability. Deleterious effect of dislocation on p-on-n double layer heterojunction diodes has been studied (ref. 2 and 3). It has been shown that at 77K, dislocation densities greater than the mid 10^6 cm^{-2} can produce dark current densities in excess of the diode diffusion current. **These studies therefore support the requirement, previously accepted, of mid 10^5 cm^{-2} or less as the suitable level in terms of dislocation density in HgCdTe material for IR photo diodes.** EPD has been so far the screening technique used to qualify HgCdTe epilayers.

Unfortunately EPD is destructive and therefore cannot be a screening technique in a manufacturing process. Thus, a non-destructive technique is required, such as DCRC, provided that a good correlation could be established with EPD count. EPIR has attempted to establish such a correlation as illustrated in Fig. 7, where the theoretical upper limit has been calculated from Gay's formula. From this curve it can be seen , as expected, that there is a general trend of a decrease in EPD when DCRC FWHM is decreased.

As discussed previously the objective in terms of EPD is mid 10^5 cm^{-2} or lower. From this curve it appears that when DCRC FWHM is not larger than 40 arcsec EPD count is mostly in the low-mid 10^5 cm^{-2} range. This correlation is clearly established on Fig. 8 which displays EPD vs FWHM for layers grown during the second and third year of this program. Incidentally the large FWHM's and EPD's reported on Fig. 7 about epilayers grown during Year I are the result of non-optimized growth conditions purposely used to study the influence of growth conditions on crystal quality as shown in Fig. 4, 5, and 6.

This study demonstrates that by using a simple, fast and nondestructive technique such as Double Crystal X-ray diffraction it is possible to screen with reliability MBE grown HgCdTe epilayers in terms of dislocation density. This represents an important contribution in manufacturing procedure. This study has also shown interesting features. The spread in EPD's for low DCRC FWHM is not understood at the present. Several parameters

such as CdZnTe surface preparation, CdZnTe lattice parameter, particle spitting from the effusion cells, minute changes in Hg flux or growth temperature are suspected and have to be investigated thoroughly. A correlation between EPD and macroscopic defect density might explain the spread., Such a correlation would be interesting to establish.

Figure 7 displays also EPD measured on epilayers grown on CdTe(211)B substrate. It appears that on CdTe substrate the best FWHM and EPD are 50 arcsec and 1×10^{6} cm^{-2} respectively. **This confirms that a lattice matched substrate such as CdZnTe is more suitable for the epitaxy by MBE of HgCdTe (x=0.22). This also suggests that if alternate substrates such as GaAs or Si are selected a CdZnTe lattice matched buffer layer should be more appropriate than a CdTe buffer layer.**

At EPIR growth parameters have been optimized in order to get on a routine basis EPD lower than 5×10^{5} cm^{-2}.

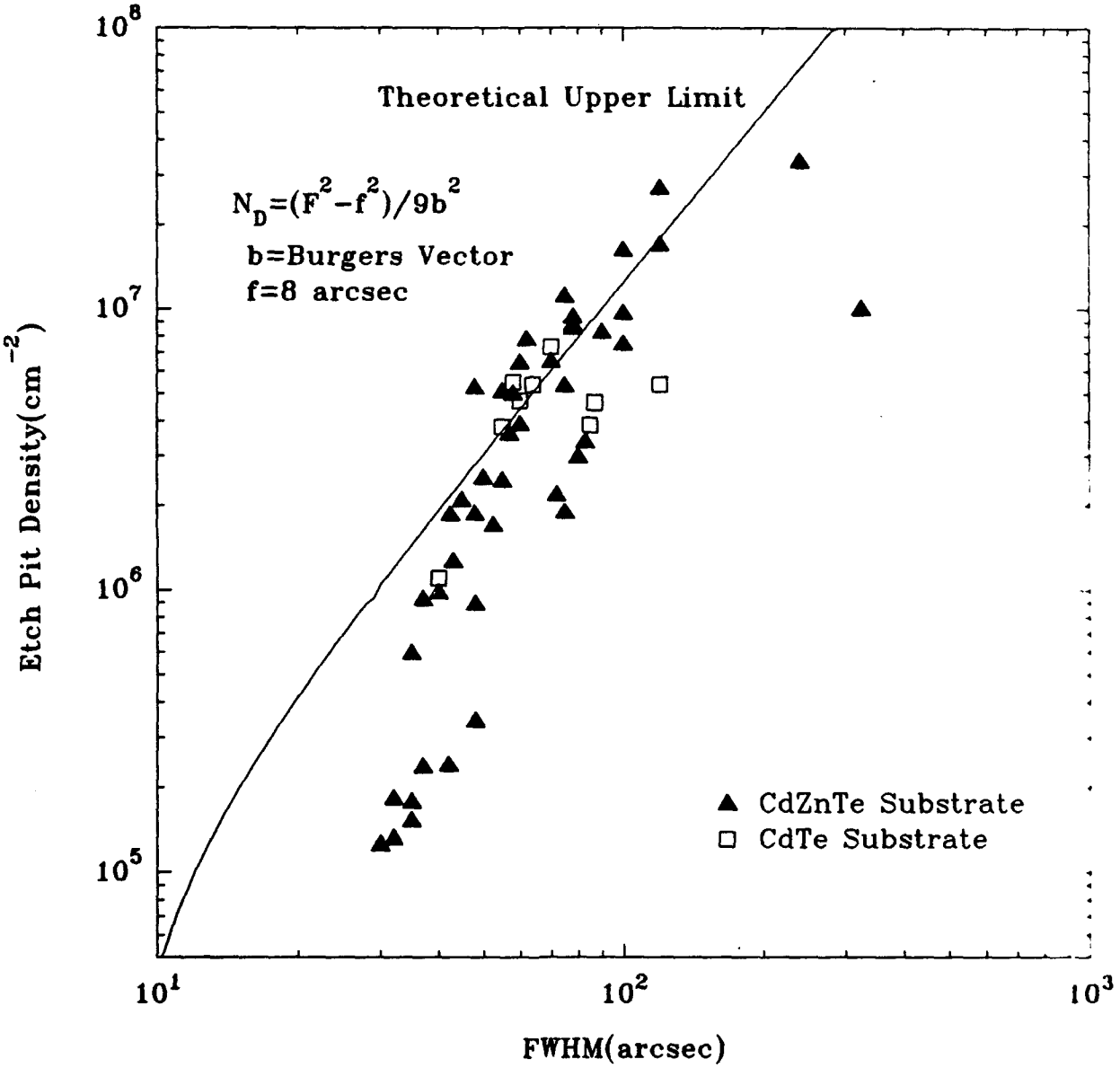
MBE (211)B HgCdTe on CdZnTe and CdTe
Theoretical Upper Limit
$N_D=(F^2-f^2)/9b^2$
b=Burgers Vector
f=8 arcsec
CdZnTe Substrate
CdTe Substrate
Etch Pit Density(cm^{-2})
FWHM(arcsec)
10^8
10^7
10^6
10^5
10^1
10^2
10^3

Fig. 7

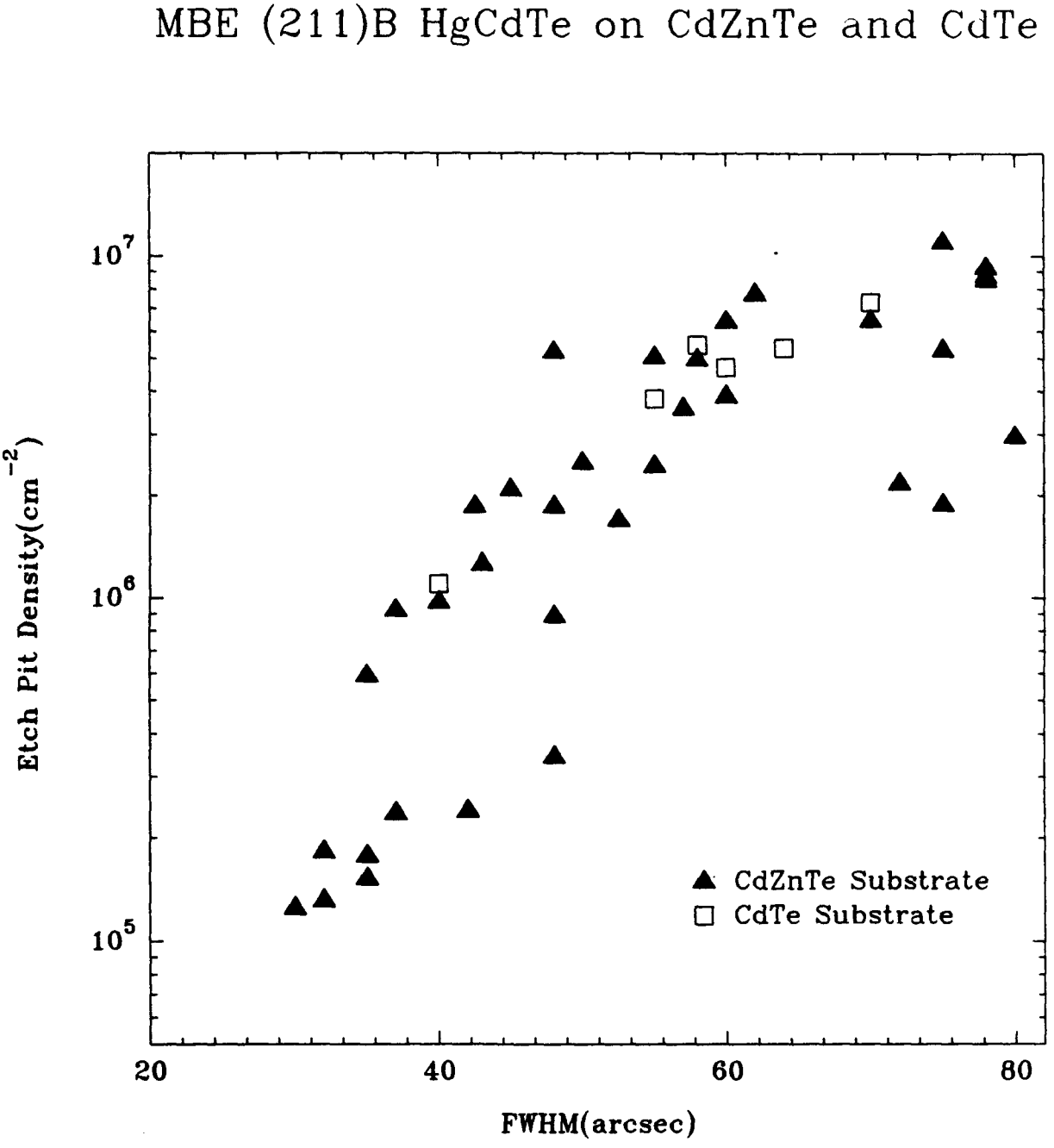
MBE (211)B HgCdTe on CdZnTe and CdTe
Etch Pit Density(cm^{-2})
10^7
10^6
10^5
20
40
60
80
FWHM(arcsec)
CdZnTe Substrate
CdTe Substrate

Fig. 8

VI ELECTRICAL PROPERTIES

Establishing the behavior of extrinsic dopants in $Hg_{1-x}Cd_xTe$ is very important. Small concentrations of unintentionally added elements can, if electrically active, affect the properties of the material and influence the performance of devices. More importantly, the need to produce photo diodes with improved performance may ultimately require intentionally doped material with known and controllable concentrations of both donor and acceptor elements on both sides of the junction.

It is obvious that undoped material, both in the as-grown and low temperature Hg-annealed states must be studied before the effect of deliberate doping can be understood. This aspect become increasingly important in an epitaxial process such as MBE where growth temperature is low. A complex picture of behavior has been described[4]. In MBE material several factors such as substrate orientation, growth temperature, Hg flux and the x value of the layer appear to influence the electrical properties.

From the early investigations it was difficult to determine what controls electronic properties between native defects (Hg vacancy, interstitial Te...) and background impurities. **In the absence of a solid understanding regarding intrinsic as well as extrinsic doping in MBE grown layers it appeared, at the initiation of this program, that investigating electrical properties of as-grown and Hg-annealed of unintentionally as well as intentionally doped material was a prerequisite to a manufacturing program.**

VI-1 DOPING OF UNINTENTIONALLY DOPED LAYERS

The doping in unintentionally doped HgCdTe layers is related to

1. Intrinsic doping from point defects (primarily Hg vacancies, Te interstitials...) and

2. Background impurities introduced during the growth and/or diffusing from the substrate.

Since the effect of these two potential sources of doping are combined their specific contribution is extremely difficult to determine. The analysis of the MBE growth conditions shows that according to P-T phase diagram $Hg_{1-x}Cd_xTe$ (x=0.22) grown at 185C should be p-type with a doping level in the high 10^{15} cm^{-3} range if doping is mainly controlled by Hg vacancies and if MBE can be considered to occur near equilibrium conditions which is still to be proven.

VI-1-1 BACKGROUND IMPURITIES

Unintentionally doped MBE as-grown layer do not always exhibit a p-type character. When EPIR started this program, erratic behavior (in terms of electrical properties) of as-grown as well as annealed MBE epilayers was observed in different laboratories, including the Microphysics Laboratory at the University of Illinois at Chicago. During the first year EPIR has found that it was not due to a lack of control in MBE growth but to diffusion of impurities from the substrate. EPIR has, in this matter and early in this program brought convincing evidences which are summarized hereafter:

- After isothermal anneal HgCdTe MBE layers should exhibit a residual background level which can be called "genuine" or "intrinsic" MBE background level. In previous studies, an understanding of the " intrinsic" doping was hindered by the presence of twins in (111)B, and the analysis of a few twin-free (111)B layers had not been conclusive[6] because of what is discussed below and unknown at that time.

- In the first annual report (Nov. 1991) we have shown that as-grown $Hg_{1-x}Cd_xTe$ ($x \approx 0.22$) epilayers grown at EPIR under similar conditions on (211)CdZnTe substrate, bought from various suppliers, displayed striking differences in carrier concentration as well as in mobilities. After isothermal anneal large differences remain. These differences have been explained satisfactorily by the diffusion, in the epilayer, of impurities originating from the substrate. SIMS analysis have been performed and impurities such as Li, Na, Ag, and Cu have been found. This problem had been observed for all the epilayers, however, the impurity level varied from supplier to supplier and even from lot to lot.

- The distribution of these impurities strongly depended upon the temperature and the duration of the anneal. It appeared that when the layer is exposed to a high temperature anneal at 400C or above the electrical behavior of the layer is improved. This effect is thought to be due to the segregation of impurities at the epilayer surface. The origin of the contamination and the role played by the tellurium precipitates are still unanswered questions.

- Experiments carried out during Year II on selected substrates of the same batch have shown that the surface of the substrate might also have accumulated impurities. For a series of NIMTEC substrates a deep etch was necessary in order to grow a clean HgCdTe epilayer. A 2 μm etch prior to growth was enough to prevent contamination from substrate surface whereas 5 μm etch was enough.

- The conclusion at EPIR is that CdZnTe(211)B substrates from NIMTEC company are still currently the best substrates commercially available. However, non-intentionally doped material grown on these substrates both in the as-grown and Hg anneal states exhibit very often mixed electrical conduction. This indicates that background impurities are competing with native defects to govern electrical properties in the low 10^{15} cm^{-3} range. The shape of carrier concentration and mobility vs 1/T curve determined from Hall measurements only can be explained by nonuniform distribution of carriers. The incorporation of indium, during growth, which is reported hereafter has been carried out not only to control mid to high donor levels but also in order to establish a background level.

However as it is discussed in detail in section VI-4 the lower limit of 2×10^{15} cm^{-3} controlled by on In-doped MBE HgCdTe is still due to impurities diffusing from NIMTEC substrates. **Substrate screening and cleaning are therefore two very important steps in a MBE manufacturing program.**

VI-1-2 INTRINSIC DOPING

With a limited impurity background it is possible to try to determine the intrinsic doping in MBE grown HgCdTe layers and to compare with the predicted intrinsic doping at equilibrium. The question has been investigated in detail during the 2nd and 3rd year of this contract. The study has been carried out on In-doped layers because it has been found that the results are very consistent. Table VIII shows the change in the acceptor level N_a between as-grown and 250C isothermal Hg-annealed states for HgCdTe material (x=0.22). A decrease of ΔN_a 5 to 9×10^{15} cm^{-3} is observed in the acceptor level. In these experiments it is also assumed that the change, if any, in N_d can be neglected compared to ΔN_a. It is generally accepted that a low temperature Hg annealing fills Hg vacancies. At 250C the concentration of Hg vacancies in a isothermal anneal being in the 10^{14} cm^{-3} range it is reasonable to conclude that this decrease in N_a concentration corresponds roughly to the Hg vacancy concentration produced during MBE growth. Actually this value ΔN_a compares well with the Hg vacancy concentration expected for a growth occurring at 185C at equilibrium under Te saturated conditions. This very important point has been investigated in much detail at EPIR only for the (211)B orientation. Since crystallographic orientation plays a major role in MBE growth especially regarding mercury sticking coefficient[5] intrinsic doping related to point defects might be very different for other crystallographic orientations. However, since all the growths performed at EPIR have been carried out in the (211)B orientation this represents a solid basis, which has never been established before, towards understanding and control of the doping.

VI-2 N-TYPE DOPING

Table VIII

Name	N_d-N_a(cm^{-3}) (as-grown)	N_d-N_a(cm^{-3}) (n-type annealed)	ΔN_d(cm^{-3})	Hg Flux (arbitary units)	x%
069	1.3×10^{16}	2.2×10^{16}	9×10^{15}	5.3×10^{-6}	24.4
070	1.8×10^{16}	2.6×10^{16}	8×10^{15}	5.5×10^{-6}	20.5
071	1.6×10^{16}	2.0×10^{16}	4×10^{15}	5.4×10^{-6}	20.5
019	1.1×10^{16}	1.7×10^{16}	6×10^{15}	5.7×10^{-6}	20.5
020	0.75×10^{16}	1.5×10^{16}	7.5×10^{15}	5.8×10^{-6}	20.5
023	0.75×10^{16}	1.9×10^{16}	9×10^{15}	5.7×10^{-6}	19.0
013	0.75×10^{16}	1.4×10^{16}	5.3×10^{15}	5.7×10^{-6}	22.0

The incorporation of indium during the growth by MBE of HgCdTe has been previously investigated in the Microphysics Laboratory and it has been found that indium is an excellent donor. Up to a level in the 10^{17} cm^{-3} range, indium has as electrical activity of almost 100%. The memory effect which has been reported in an earlier study is currently under control.

Indium-doped HgCdTe epilayers have been grown at EPIR during year II and Year III under optimized MBE growth conditions on (211)B CdZnTe substrates in order to establish the lowest n-type background possible, to measure the epilayers characteristic and to analyze the favorable effect of indium. In-doped layers after a n-type anneal exhibit excellent electrical properties. Electron mobilities ranging from 2-4$\times 10^5$ $cm^2/V.sec$ at 23K are particularly outstanding and compared well with the best mobilities ever reported for HgCdTe with this cadmium composition (Fig. 9).

At the end of Year II the lowest controlled level was 3×10^{15} cm^{-3}. During Year III we have been able to lower this level down to 2×10^{15} cm^{-3}.

From Hall measurements performed on each as-grown and annealed epilayers they, can be classified into three categories (Fig 10).

1. Carrier concentrations (CC) $N_d - N_a \geq 2 \times 10^{15}$ cm^{-3}

   Electron mobility decreases when CC increases which is expected.

2. Carrier concentration $\leq 1 \times 10^{15}$ cm^{-3}

   Electron mobility decreases when CC decreases which indicates that compensation occurs.

3. Carrier concentrations (CC) 1×10^{15} $cm^{-3} < N_d - N_a < 2 \times 10^{15}$ cm^{-3}

   Electron mobility is almost constant.

A doping level of 2×10^{15} cm^{-3} is low enough and very appropriate for current IR photodiode applications. The targeted doping level on LPE production line is currently 3×10^{15} cm^{-3} [1]. However, CC in the mid 10^{14} cm^{-3} with minority carrier lifetime of several microseconds have been reported for LPE HgCdTe material. Hence, it is important to determine what prevents MBE material to exhibit such a low doping level. Mobility vs N_d trend which is illustrated in Fig 10 will be correlated with minority carrier lifetime in the following section.

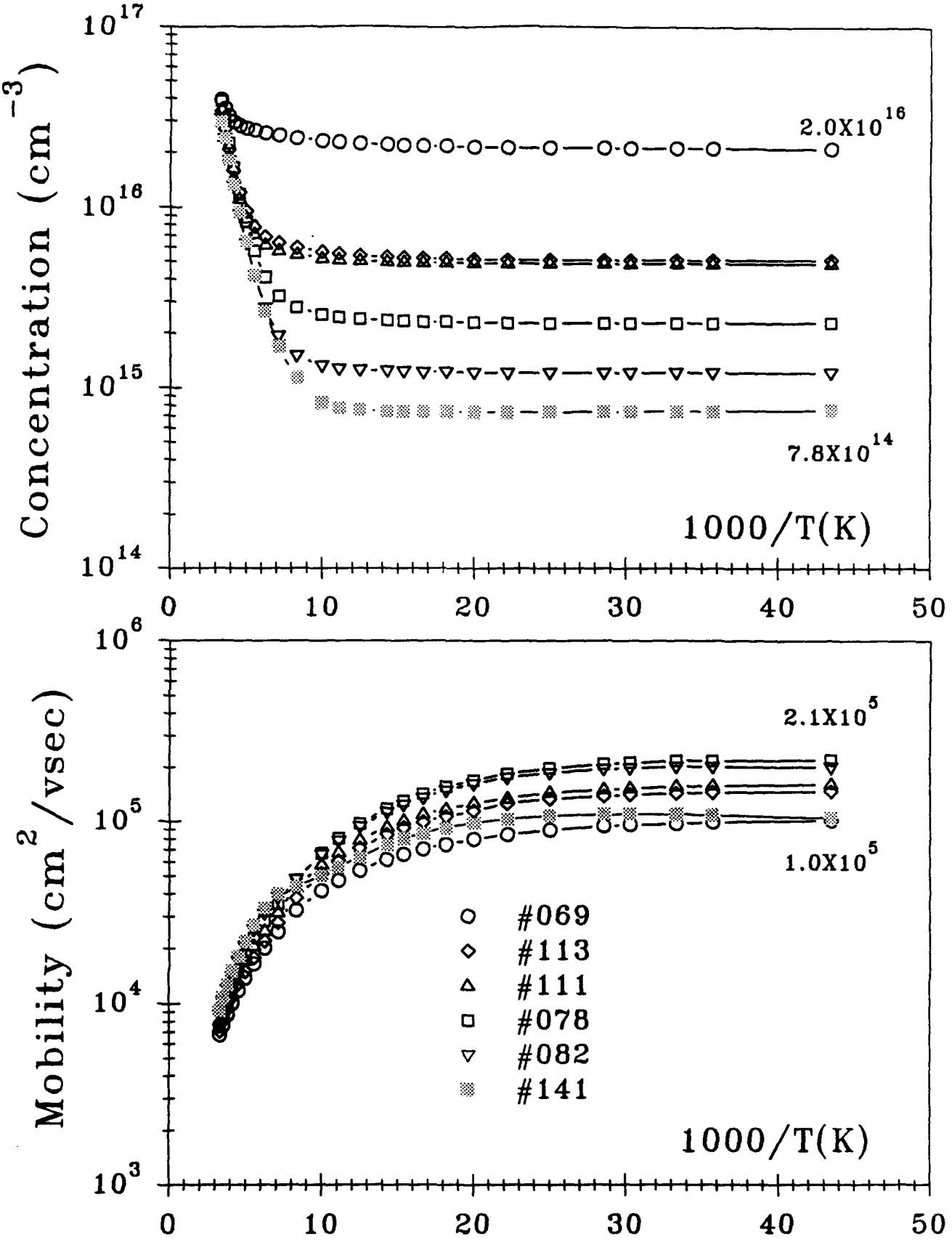

Fig. 9 Carrier concentration vs reciprocal temp. for (211)B indium-doped MBE grown layers.

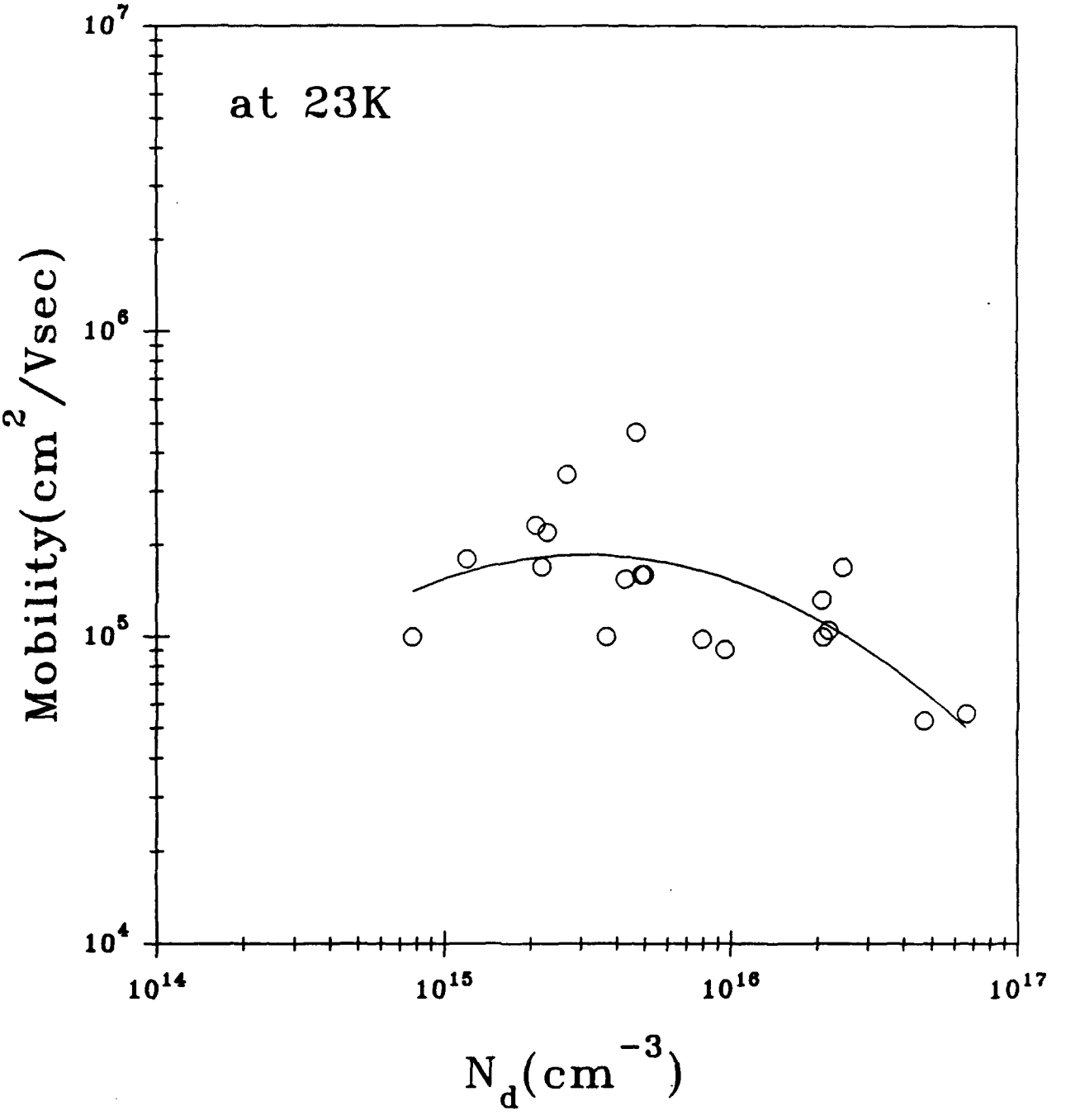

Fig. 10 Mibility vs doping level at 23K.

VI-3 MINORITY CARRIER LIFETIME OF INDIUM DOPED MBE GROWN HgCdTe

During Year III minority carrier lifetime(τ) of In-doped epilayers grown at EPIR has been thoroughly investigated since this electrical parameter is of extreme importance in the performance of infrared detectors[7]. It is essential to understand the factors that limit the recombination mechanism in MBE-grown layers. Electron lifetime on (111)B p-type HgCdTe layers grown by MBE has been previously reported[8]. The temperature dependence of the lifetime on these p-type HgCdTe layers was explained in terms of the Schockley-Read (SR) recombination mechanisms in the extrinsic temperature region and have shown a deep level closer to midgap. Lifetimes on *n*-type HgCdTe were studied by several investigators,[9–11] but layers were grown by different growth techniques. In the bulk grown crystals, lifetime follows at low temperatures band-to-band recombinations. This included Auger, radiative or both contributions. Compensated layers show SR recombination. Reported energy levels ranging from 10 to 70 meV below the conduction band. On epitaxial layers very little work has been reported in literature.

All of the layers investigated were annealed under Hg-saturated atmosphere at 250C in order to reduce the Hg-vacancy concentration created during the MBE growth. The carrier concentration and the mobility of the layers were measured by the van der Pauw technique for temperatures ranging from 300K to 20K and magnetic fields up to 1.0 Tesla. The lifetime measurements were carried out using the photoconductive decay technique. All the samples were etched in Br-methanol solution prior to measurement. This is very important, since we do not passivate our samples after the anneal at 250C. A pulsed GaAlAs laser beam (λ=850 nm) was focused on the sample to generate the excess carriers. The samples were mounted on the cold finger of a liquid nitrogen variable temperature dewar. Indium was used to make good ohmic contacts for n-type layers.

Minority carrier lifetime in *n*-type HgCdTe is determined by several different recombination mechanisms; namely Auger, radiative, and Schockly-Read mechanisms and these have been discussed extensively in the literature.[9,12,13] We have applied all these mechanisms for MBE-grown,

indium-doped, HgCdTe layers.

LIFETIME VERSUS TEMPERATURE

Measured lifetime and material parameters of these annealed indium-doped *n*-type layers at 80K are summarized in Table IX. These indium-doped layers show excellent electrical properties as previously discussed (See Figs 9 and 10). N_d is the doping concentration extracted from the measured $R_h(T)$ data at B=0.4 Tesla and n is the equilibrium electron concentration extracted from lifetime. Figure 11 shows the lifetime versus reciprocal temperature from three selected layers from Table IX in an increasing order of the doping level. Symbols represent experimental data points. It can be seen that, as the temperature decreases, the lifetime increases, becomes maximum, and then decreases. The peak lifetime reaches $\approx 1.4\mu$sec at 130K, and at lower temperature it decreases exponentially. For the highest doping level, maximum τ reaches $\approx$ 100 nsec. The solid lines represent the theoretical curves, which include only Auger and radiative recombination processes (see Fig 11) The value of the doping concentration (n_0) obtained from the fitting of τ data are also shown in Table IX. As can be seen, there is an excellent correlation between the experimental data and the intrinsic material properties of MBE-grown HgCdTe layers. Similar behavior is obtained for higher doping levels, up to $\approx 1.0 \times 10^{16}$ cm^{-3}. The Auger lifetime dominates throughout the entire temperature region down to 80K.

However on the other hand when the doping is low for some of the MBE-grown layers cannot be explained only by intrinsic properties. In these cases lifetimes data cannot be fully fitted using only band-to-band recombination processes. In order to obtain a good fit throughout the entire temperature range we had to assume recombination from SR centers in addition to the combined Auger and radiative processes. Table X shows the measured lifetime, transport properties, and material parameters on some of these layers at 80K. **It appears that this behavior dominates when the doping level falls below $\approx 2.0\times10^{15}$ cm^{-3}.** Also, Table X contains the values of E_t and τ_{p0} obtained by fitting to the experimental data according to the theory. The SR energy level E_t varies between 33 and 45 meV below the conduction band on these layers, as can be seen from the table.

As an example, Figure 12 shows lifetime versus reciprocal temperature for sample #82, which

Table IX

Sample Name	x (%)	t (μm)	N_d (cm^{-3}) [Extracted from $R_h(T)$] ($\times 10^{15}$)	μ ($cm^2/V.s$) at 23K ($\times 10^5$)	n_0 (cm^{-3}) [Extracted from lifetime] ($\times 10^{15}$)	τ at 80K (nsec)
139	21.7	08.7	1.4	1.6	1.3	940
075	22.0	10.3	2.0	2.3	1.8	580
078	22.0	10.8	2.3	2.2	2.7	410
077	22.2	11.4	2.2	1.3	2.9	220
072	23.7	11.5	4.0	1.6	3.1	250
113	22.6	12.1	4.7	1.6	3.3	184
111	22.0	12.2	4.9	1.6	3.6	140
069	24.4	09.5	21.0	1.0	11.0	20

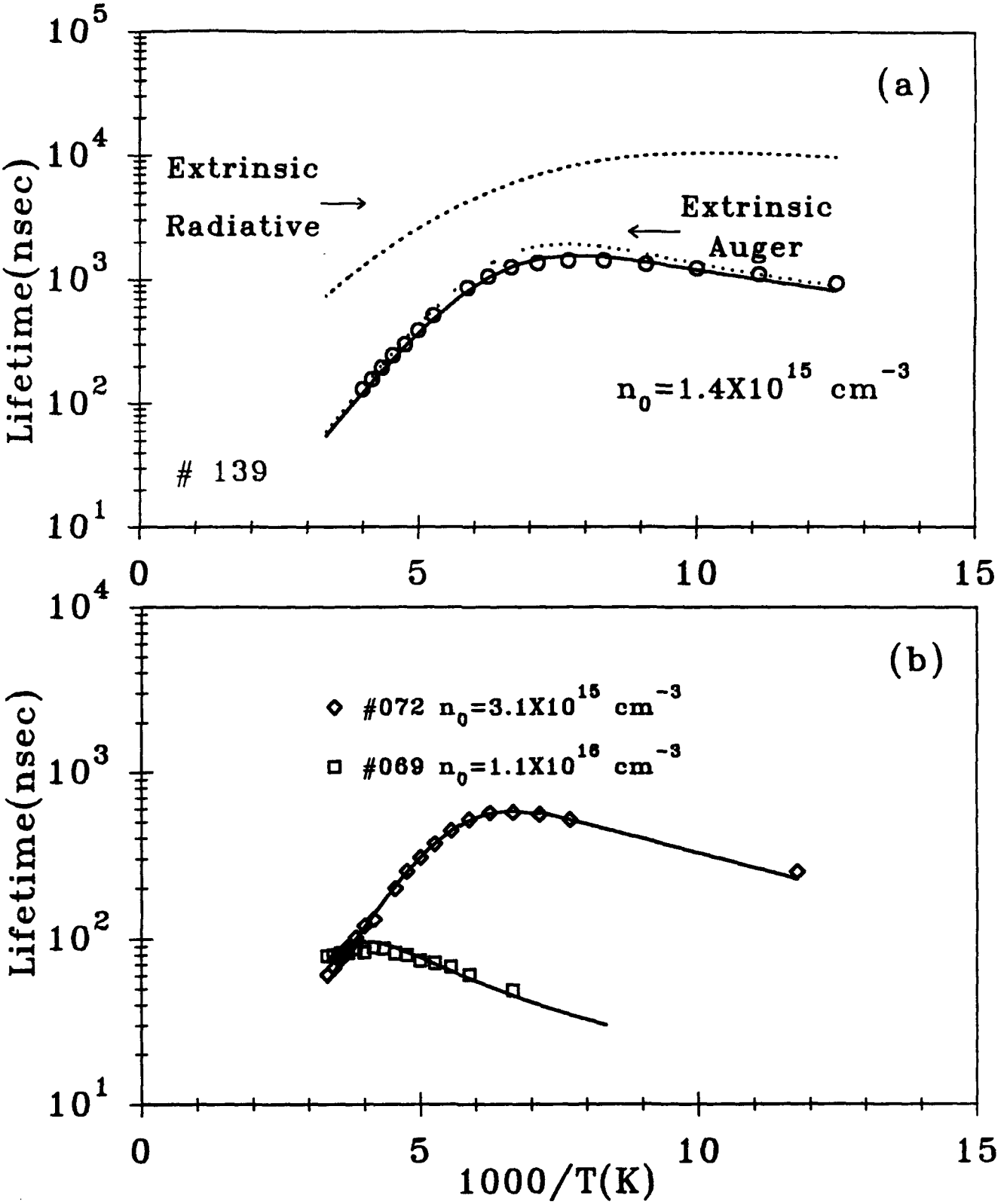

Fig. 11 Measured and theoretical minority carrier lifetime on low and high indium doped MBE grown HgCdTe layers. Solid lines show the combined contribution from Auger plus radiative recombination processes.

Table X

Sample Name	x (%)	N_d (cm^{-3}) [Extracted from $R_h(T)$] ($\times 10^{15}$)	n_0 (cm^{-3}) [Extracted from lifetime] ($\times 10^{15}$)	τ at 80K (nsec)	E_t (meV)	τ_{p0} (nsec)
082	22.1	1.4	1.4	780	45.1	8900
073	24.6	3.8	2.7	560	32.7	7800
044	24.5	1.9	1.9	235	40.2	9500
074[annealed]	25.4	1.4	1.0	1490	38.6	6063
074[as-grown]	25.4	1.6	2.0	150	44	162

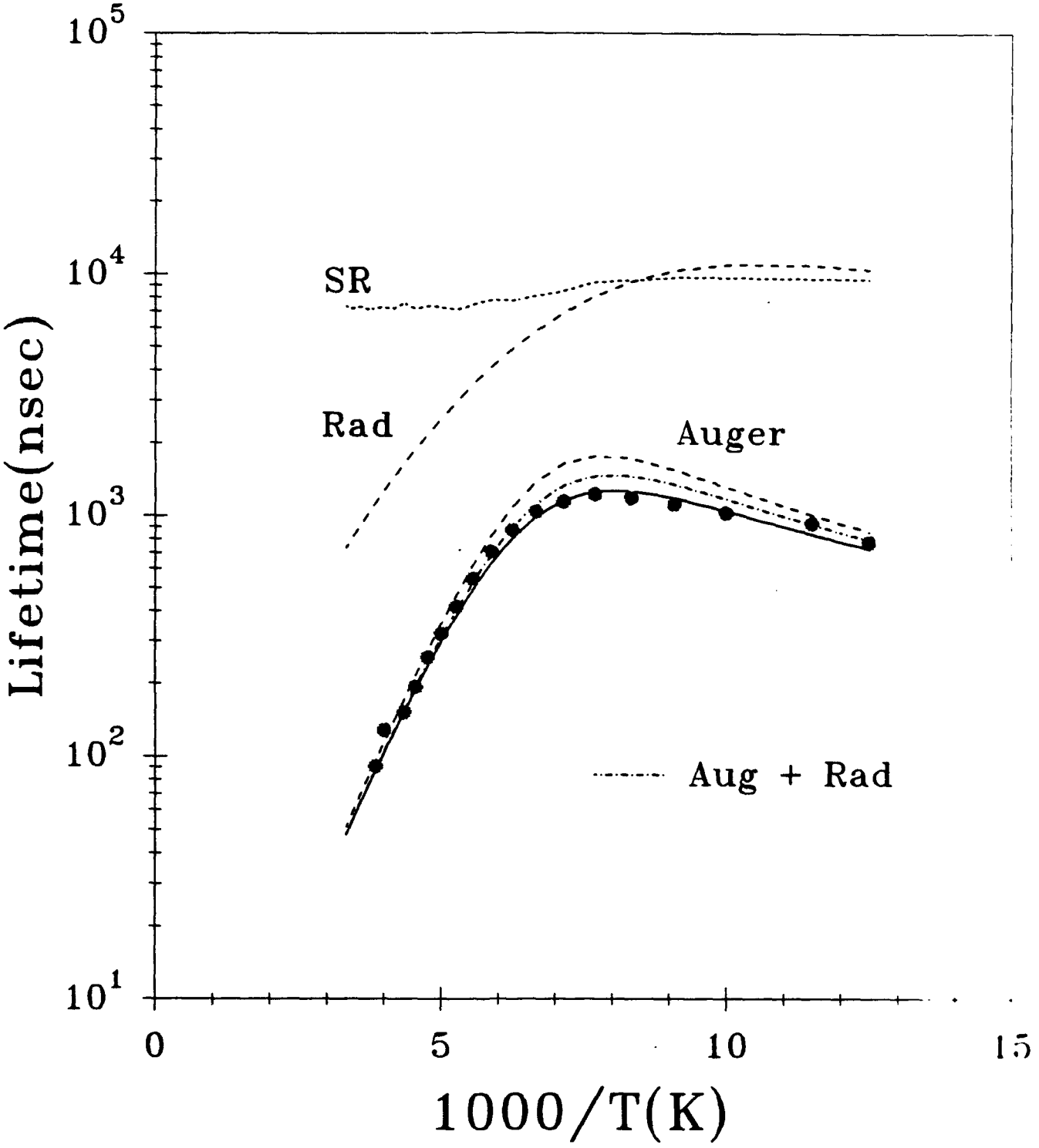

Fig. 12 Dependence of minority carrier lifetime vs reciprocal temp. on layer #82.

falls into this category. It is evident that the behavior is very similar to those samples in Fig 11. The combined Auger and radiative lifetime gives good agreement with the experimental data in the intrinsic temperature region. But, in the extrinsic temperature range the data is lower by a factor of $\approx$ 1.2 than the theory. Hence, in order to obtain a good fit throughout the entire temperature range, we had to assume recombination from SR centers in addition to the combined Auger and radiative processes.

In order to find out the origin of this defect level, we carried out lifetime measurement on as-grown, indium-doped, sample #74. The measured lifetime was again lower than the band-to-band recombination lifetime at temperatures below 200K. At 80K, lifetime is $\approx$ 150nsec. Figure 13b shows the lifetime data on the same sample after it was annealed at 250C under Hg saturated conditions. Note that lifetime improved from 150 nsec to 1.4 μsec at 80K. This is an improvement of almost one order of magnitude. The solid line represents the best fit curve, and it was obtained with all recombination mechanisms as discussed previously. During MBE at a growth temperature of 185C, it is very difficult to avoid compensation due to Hg vacancies, especially when the indium doping levels are in the range of 10^{15} cm^{-3} (we assume that N_d arises mainly from indium atoms). At 185C, according to the HgCdTe P-T phase diagram as already discussed, the acceptor level due to Hg vacancies should be also in the 10^{15} cm^{-3} range. Hence, as-grown layers are very compensated.

For layer #074 in the as-grown state, we obtained $N_d = 1.6\times10^{15}$ cm^{-3} and $N_a = 1.5\times10^{15}$ cm^{-3} from fitting of R_h(T) versus temperature data. After n-type annealing under Hg pressure, we obtained $N_d = 1.4 \times 10^{15}$ cm^{-3} and $N_a = 1.4 \times 10^{14}$ cm^{-3}. From the lifetime data, τ_{p0} increased from 162 nsec to 6 μsec when N_a decreased from 1.5×10^{15} cm^{-3} to 1.4×10^{14} cm^{-3}. According to Figure 11, this SR defect level was not seen for doping levels up to 1.0×10^{16} cm^{-3} (which does not mean that it has disappeared). Since these samples were indium-doped during the growth, it is safe to assume that the origin of this SR defect level is not related to extrinsic indium. **Hence, we concluded that this SR level is somehow related to the Hg vacancies.** It should be pointed out that if this level is Hg vacancy related its concentration is the same in all In-doped layers since Hg-annealing conditions are the same. However, the correction factor of 1.2 for layer # 082 should decrease when N_d increases (τ decreases) and therefore it can be neglected which explains why this

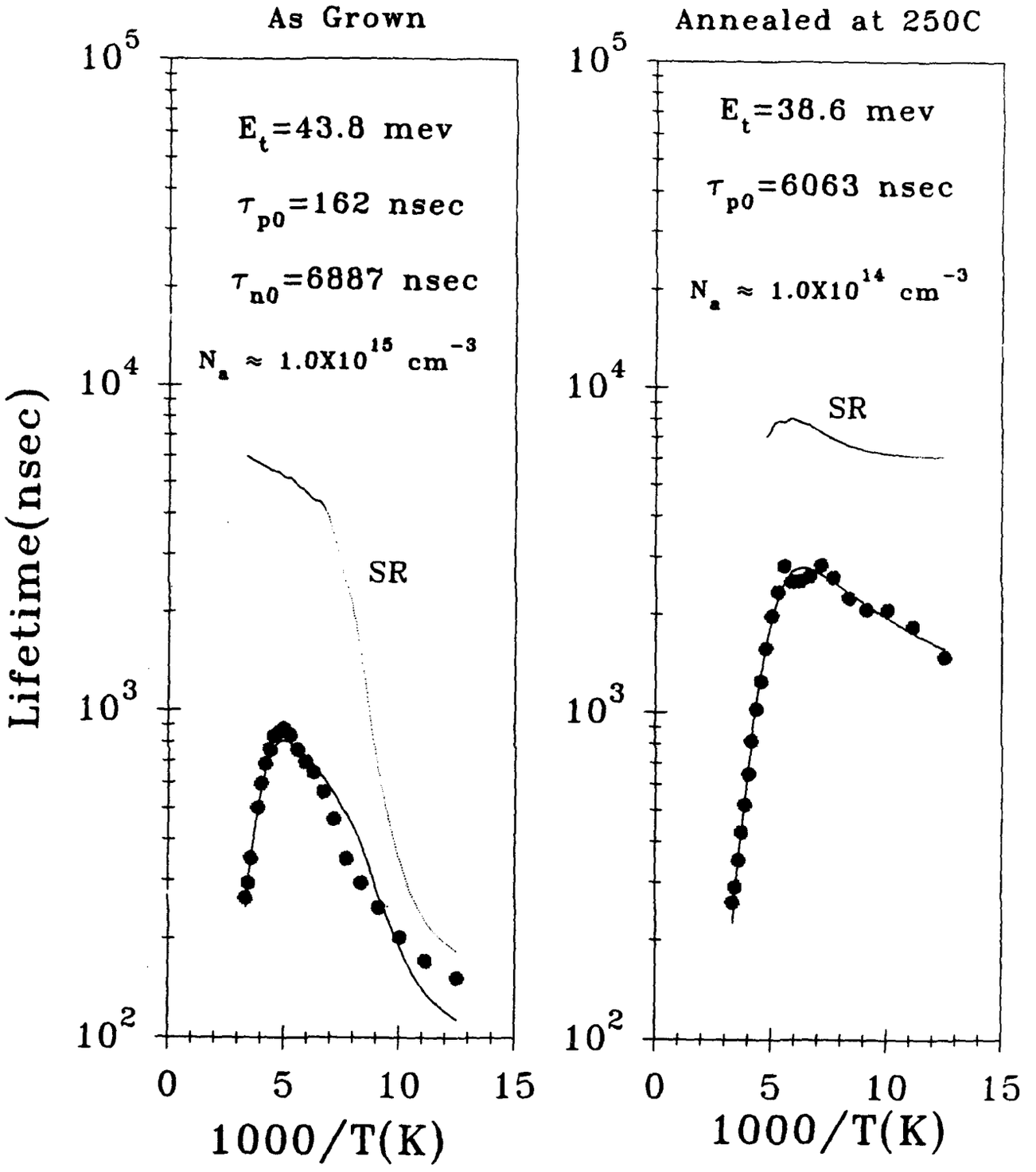

Fig. 13 Measured and theoretical minority carrier lifetime vs reciprocal temperature on layer #74

SR level "is not seen" in layers with higher doping levels.

Lifetime versus Electron Concentration

Figure 14 shows the behavior of the lifetime versus electron concentration of indium-doped HgCdTe layers at 80K. Lifetime decreased from ≈ 950 nsec to ≈20 nsec when doping increased from ≈1.4×10^{15} cm^{-3} to ≈1.0×10^{16} cm^{-3}. The solid line shows n_0^{-2} dependence, as expected; and this further confirms that the measured lifetime is limited by Auger recombination in the extrinsic temperature region. We have taken $|F_1F_2|$ to be 0.22, for Cd composition 0f 22%. Since there exists an ambiguity in the exact value of $|F_1F_2|$ for HgCdTe in the literature[9,10,13], we have also calculated the concentration dependence of lifetime for upper and lower limits of $|F_1F_2|$. The lifetime data follows extremely well for $|F_1F_2|$=0.22, and the inverse square dependence of the electron concentration is clearly visible.

VI-4 DISCUSSION RELATED TO DOPING LIMITATION IN MBE GROWN LAYER

From electrical measurements it clearly appears that doping level in n-type Indium-doped MBE grown HgCdTe layers is controlled down to only 2×10^{15} cm^{-3}.

$\underline{N_d < 2.0 \times 10^{15}\ cm^{-3}}$

Below 2.0×10^{15} cm^{-3} compensation occurs. Mobility and carrier concentration vs 1/T curves does start to reflect non uniformity in carrier distribution.

As can be seen in Fig 9 there is a shoulder on the mobility curve around 80K of the layer # 141 exhibiting $N_d - N_a$=7.8×10^{14} cm^{-3}. Minority carrier lifetime vs 1/T curves require SR center(s) to be fitted.

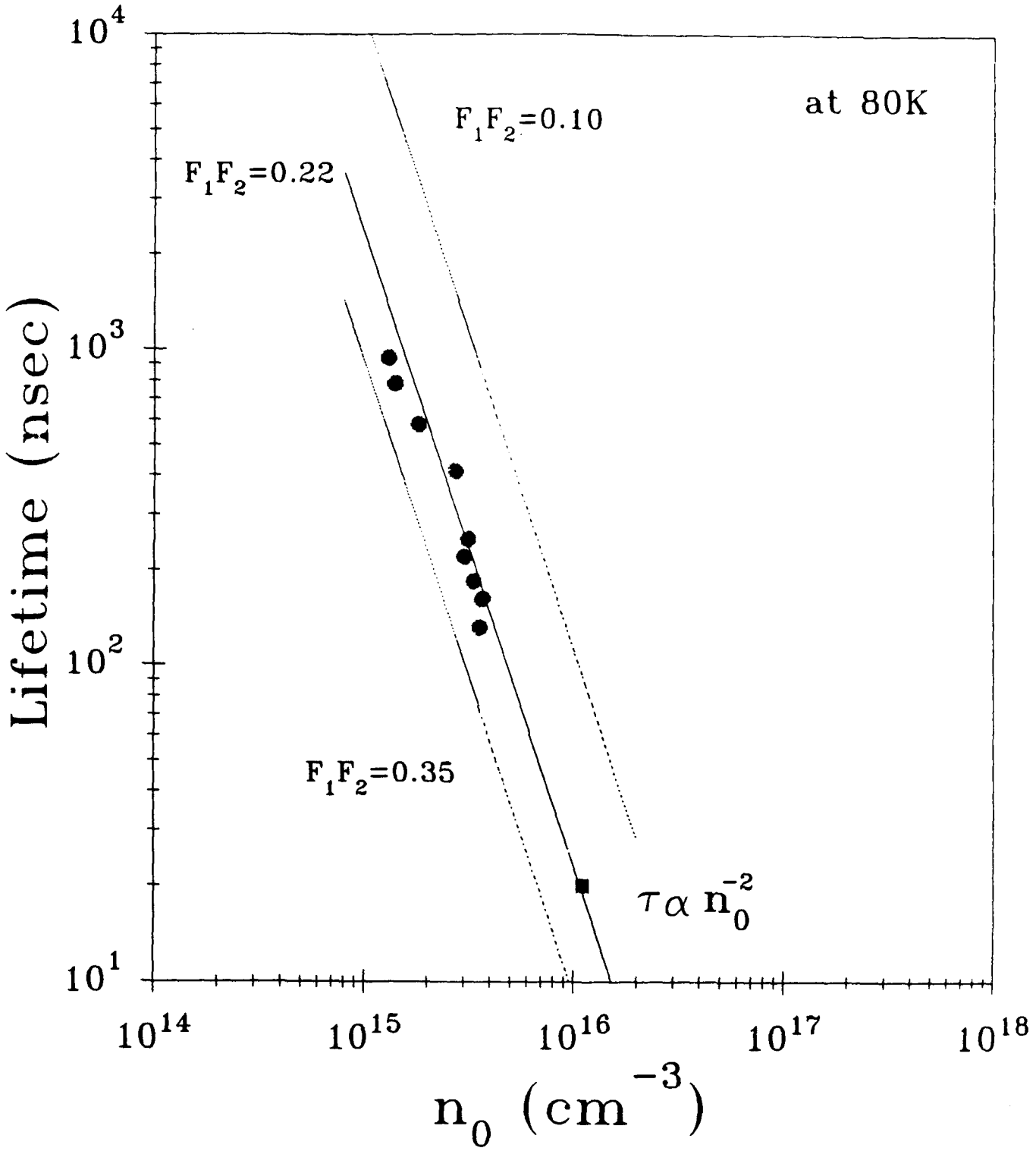

Fig. 14 Lifetime versus electron concentration of MBE-grown indium-doped $Hg_{1-x}Cd_xTe$ layers (x 22.0%).

$N_d > 2.0 \times 10^{15}$ cm^{-3}

Electrical properties are fully explained by intrinsic properties. Mobility and minority carrier lifetime increase as expected when carrier concentration decreases. SR center(s) is not required to fit lifetime vs 1/T curves.

The current lower limit of 2.0×10^{15} cm^{-3} observed in layers grown at EPIR might be controlled by impurities, point defects, Te precipitates or extended defects. No relation between lower limit and EPD's count has been observed so far. However it appears to be extremely important to investigate thoroughly this point in order to understand the origin(s) of this limit and to control the background doping in the 10^{14} cm^{-3} range. Lowering the doping level for MBE grown material is not just an academic challenge since it implies an understanding and control of residual background impurities as well as induced MBE grown defects. Lowering the level might also be important for advanced devices and low background applications. There is certainly a relation between this lower level limit and the non-uniformity problems observed in the performance of large devices operating at low temperatures.

As pointed out earlier, compensation from Hg-vacancies does show up for low-doped as grown layers and as well as low-doped annealed layers at 250C. Hence, these layers were annealed at 150C, in order to reduce further the Hg vacancy concentration down to 1×10^{12} cm^{-3}. We concentrated in this experiment more on the low doped-layers which mostly show SR recombination in the extrinsic temperature range. Table XI displays the changes in electrical data for epilayers annealed at 250C and post annealed at 150C.

As it can be seen for **all the layers** the carrier concentration N_d-N_a **increases** after the 150C anneal. This should indicate that compensation is reduced as expected since N_a is drastically reduced. Therefore both electron mobility and minority carrier lifetime should <u>increase</u>.

From Table XI it is clear that a <u>decrease</u> is measured in electron mobility for all the layers. For layers with $N_d - N_a < 2\times10^{15}$ cm^{-3} such as #82 and 139(Fig 15) the mobility is drastically reduced compared to those exhibiting a carrier concentration above 2×10^{15} cm^{-3} (Fig 16). Minority carrier lifetime is also reduced after a post anneal at 150C as illustrated in Fig 17 for layer #139.

Table XI: Summary of the measured and fitted parameters of MBE-grown $Hg_{1-x}Cd_xTe$ layers that were studied at 150C.

Name	at 250C			at 150C		
	N_d (cm^{-3})	N_a (cm^{-3})	μ at 80K (cm^2/vs)	N_d (cm^{-3})	N_a (cm^{-3})	μ at 80K (cm^2/vs)
077	2.4×10^{15}	4.8×10^{14}	7.6×10^{4}	3.1×10^{15}	1.0×10^{12}	5.4×10^{4}
078	3.0×10^{15}	7.4×10^{14}	9.7×10^{4}	2.9×10^{15}	8.2×10^{13}	8.8×10^{4}
139	1.9×10^{15}	5.0×10^{14}	7.0×10^{4}	2.1×10^{15}	1.0×10^{12}	4.5×10^{4}
075	2.3×10^{15}	1.2×10^{14}	9.5×10^{4}	2.7×10^{15}	1.8×10^{13}	8.6×10^{4}
082	1.4×10^{15}	2.0×10^{14}	9.1×10^{4}	-	-	1.6×10^{4}
069	-	-	5.1×10^{4}	-	-	5.3×10^{4}

The shoulder observed on the mobility curve (Fig 15) slightly visible after the anneal at 250C is much more pronounced after the post anneal at 150C. **This is a clear evidence of an increase in the non uniformity of the carrier distribution.**

In addition, the fitting of lifetime τ vs 1/T after the 150C post anneal requires a larger concentration of SR centers to be fitted and the energy level seems different (this has to be confirmed) than Hg-vacancy related SR centers. **Diffusion of impurities from the substrate appears to be the best hypothesis which can explain these experiments.** Therefore even after careful screening it seems that CdZnTe from NIMTEC are still source of contamination for HgCdTe epilayers grown by MBE. From these experiments two conclusions can be drawn:

1. **N_d-N_a= 2×10^{15} cm^{-3} is certainly not the lower limit achievable in terms of doping in HgCdTe grown by MBE and**

2. **In order to break this lower limit better substrates have to be grown by manufacturers and/or a specific process has to be implemented.**

For example at EPIR it has been observed that a HgCdTe epilayer grown on a substrate which has already been used(growth of HgCdTe and etching of the epilayer) exhibit better characteristics. This has already been discussed in section VI-1. The first epilayer act as a getter for impurities. However such a cleaning process is obviously not cost effective and in addition does not completely prevent diffusion of impurities if various anneals are performed. **Nevertheless, from experiments it can concluded that EPIR control, on a routine basis, electrical properties in MBE grown HgCdTe suitable for IR photodiodes i.e. doping level lower than 3×10^{15} cm^{-3} and minority carrier lifetime of 0.5 μs or larger. The results obtained are better than expected goals.**

VI-5 P-TYPE DOPING

In HgCdTe p-type doping can be controlled either by Hg vacancies and/or electrically active impurities.

Table XII

Characteristics of p-annealed In-doped HgCdTe (x=0.22) grown by grown by MBE obtained on a regular basis by EPIR Ltd.

DCRC FWHM	$\leq$ 35 arcsec
EPD	$\leq 5\times10^{5}$ cm^{-2}
23K Carrier Concentration	$\leq 1\times10^{15}$ cm^{-3}
23K Hole Mobility	$\geq$ 600 cm^{2} V^{-1}s^{-1}
77K Minority Carrier Lifetime	$\geq 0.5\times10^{-7}$ sec

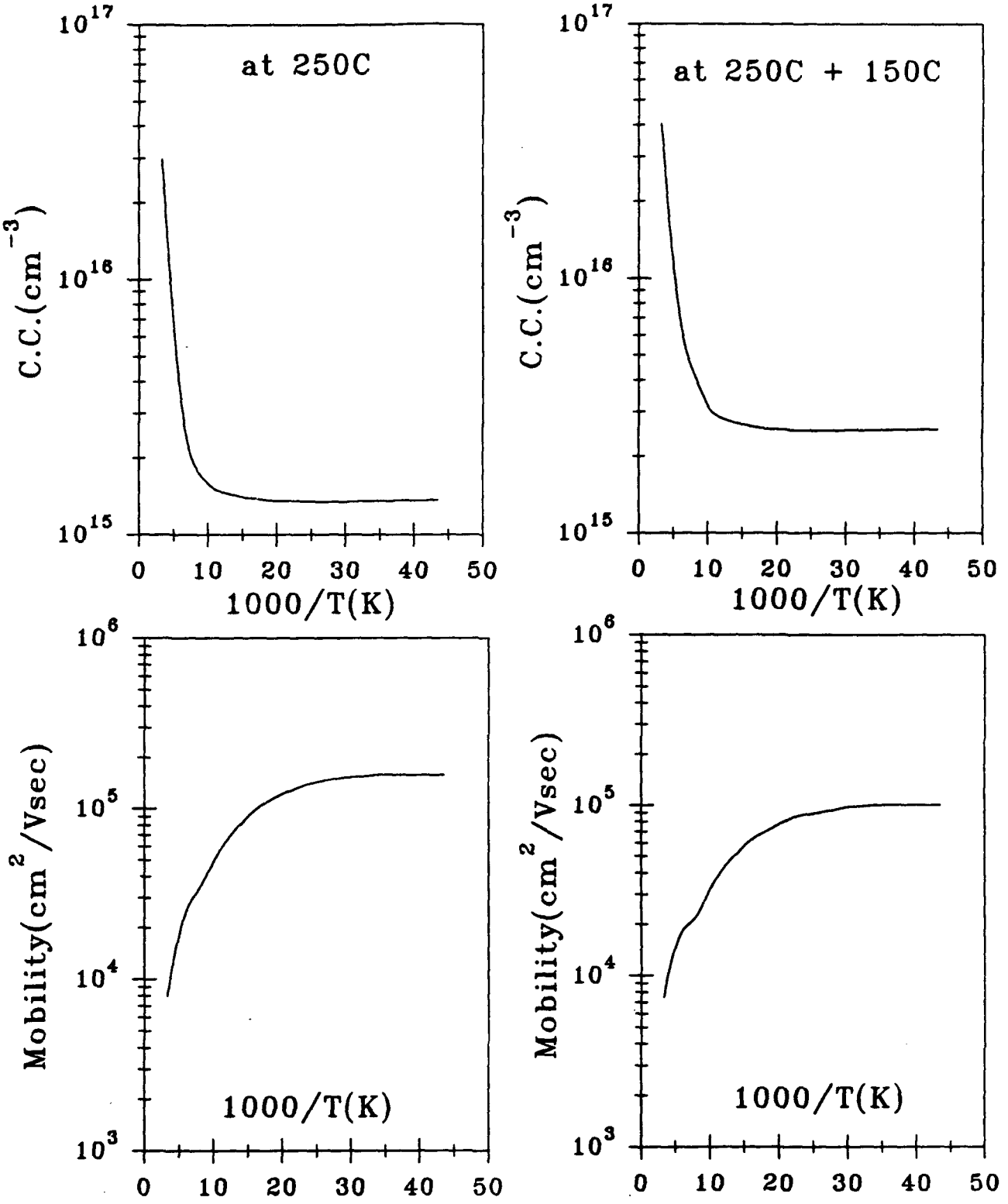

Fig. 15 Measured carrier concentration and mobility versus reciprocal temperature on layer #139 under different annealing conditions.

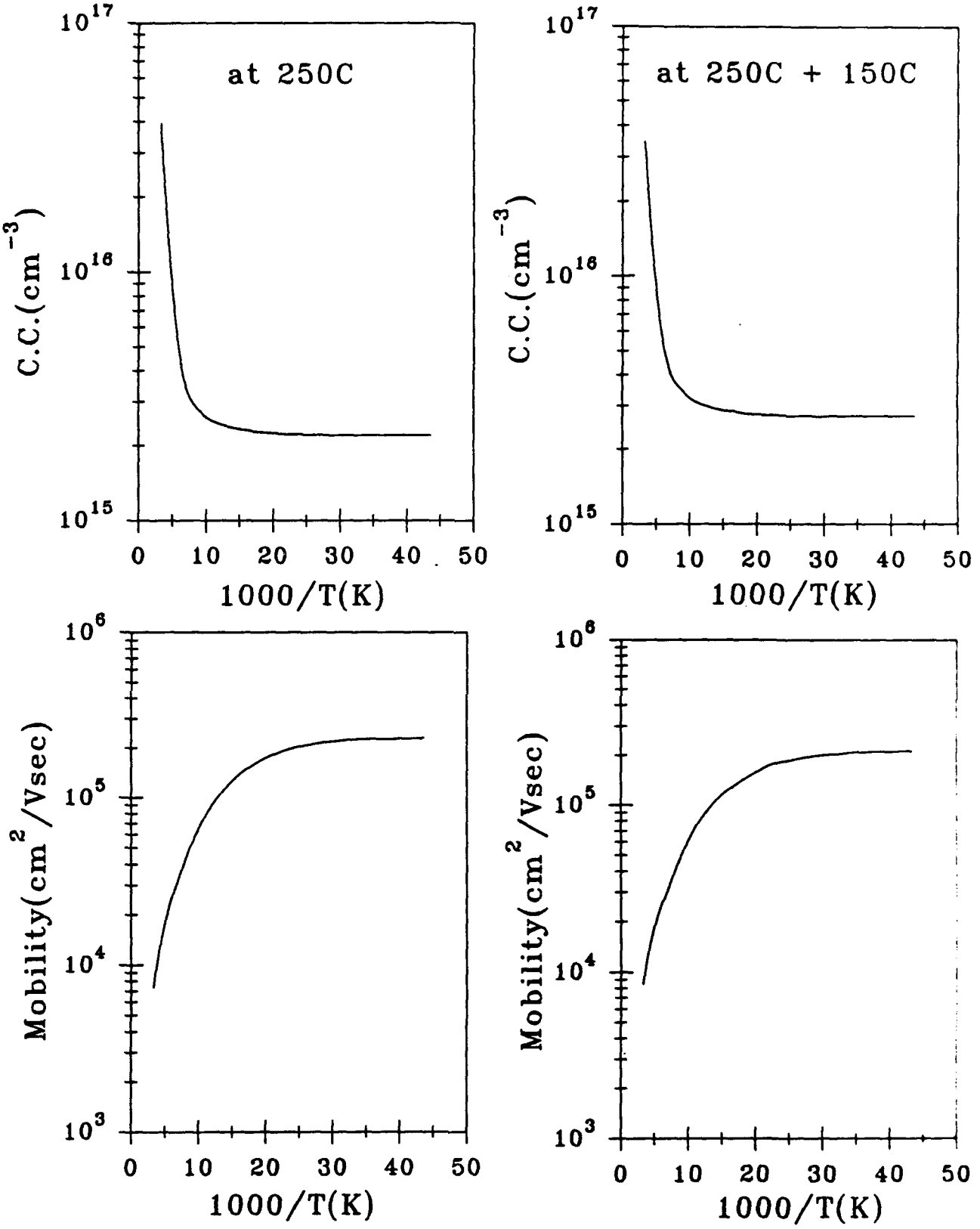

Fig. 16 Measured carrier concentration and mobility on layer # 078 under different annealing conditions.

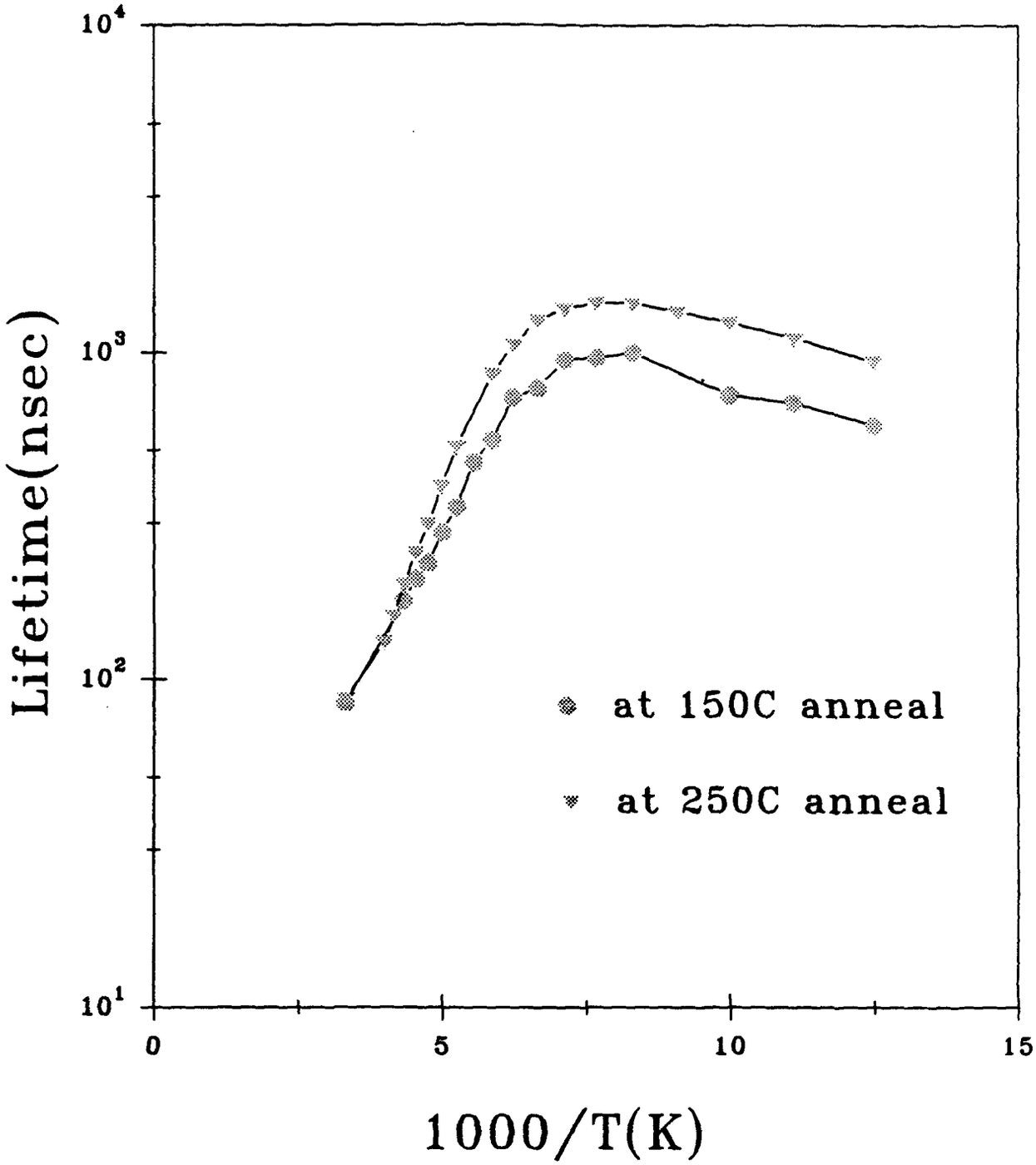

Fig. 17 Measured minority carrier lifetime on layer #139 under different annealing conditions.

VI-5-1 Hg-VACANCIES

Table XII displays the electrical characteristics of p-type annealed In-doped HgCdTe layers obtained on a regular basis at EPIR Ltd. These p-type single layers exhibit characteristics better to those presented in the program goals. In particular, lifetimes at 80K are usually between 50 and 100 nsec which is considered to be very good for Hg vacancy doped p-HgCdTe. Both mobility and carrier concentration are excellent. These p-type layers are suitable to fabricate n-on-p photodiodes either by Hg diffusion or ion implantation.

However, p-on-n junction is currently the preferred structure by U.S. manufacturers because they offer significantly better performance than n-on-p junctions for LWIR photodiodes[14]. One important advantage of this configuration is the easier control of low doping (10^{15} cm^{-3} range) in the n-type base layer than in the p-type base layer for the n-on-p junction. therefore longer minority carrier lifetime is achieved in n-type base layer. The p-side which is a capping layer of $x \approx 0.30$ should have an acceptor level in the 10^{17} cm^{-3} range. This requires the use of extrinsic dopant such as arsenic which is a slow diffusing dopant. There is also some evidence that As doping can improve lifetimes.

VI-5-2 ARSENIC DOPING

Arsenic, which is the selected impurity for extrinsic p-doping in HgCdTe, is relatively well controlled in LPE thanks to a growth temperature exceeding 450C, which has been found to be necessary to activate arsenic. Currently, in MBE there is not a satisfactory approach allowing the control of As-doping during the growth process itself. The complete activation of As is As-doped, As-diffused or As ion-implanted HgCdTe epilayers requires annealing at high temperatures of 400C - 450C for 10-30 minutes. For example after such an anneal As in situ doped HgCdTe(x=0.32) epilayer exhibits CC of 7×10^{17} cm^{-3} and hole mobility at 80K of 150 $cm^2v^{-1}s^{-1}$. This kind of anneal is detrimental to any structure which requires a precise compositional and/or doping profile.

In addition, anneal induce impurity diffusion as discussed in part from the substrate which is

highly undesirable.

As DELTA DOPING

At EPIR we had the goal of achieving p-type doping of HgCdTe with As without using any thermal process exceeding 250C. During Year II and Year III, 24 runs were carried out using a new approach, i.e. planar doping called also delta doping applied for the very first time to HgCdTe at EPIR. In this approach, periodically CdTe and Te effusion cell shutters are closed and arsenic effusion cell shutter is open. Mercury atoms are still impinging on the surface which is expected to favor Hg-As bonding.

The characteristics of this As-delta doped HgCdTe epilayers including the period are reported in Table IV whereas electrical characteristics of as-grown and annealed epilayers are presented in Tables V and VI. All these As-doped layers have been grown under different growth conditions. It is interesting to note that layer #101 exhibits p-type doping in the high 10^{16} cm^{-3} level even before any anneal is performed (Fig. 18). This is clearly one order of magnitude larger than intrinsic doping related to Hg-vacancies as expected for undoped layer. The fact that almost no freeze out is observed is also an evidence of a 2D character and a physical separation between holes and acceptor ions. **Therefore, this attests for the incorporation of As as an active acceptor at the growth temperature.**

Isothermal anneals at 250C and 300C confirm without any ambiguity that the p character is related to the presence of As and that As has been mostly activated at 185C which is the growth temperature. P-type character has been also observed for layers #92,96,106,117,119,123, and 124. However layer # 96 has a low mobility before and after anneal, layers #117 and 124 are p only before anneal whereas layers #106,119, and 123 exhibit very high hole mobilities in the as-grown state.

The other layers are n-type both in the as-grown and annealed states. It is note worthy that in some as-grown layers electrons and holes have high mobility which disappears after anneal. This is very likely related to the modulation of the As doping. This should be analyzed in more detail.

Fig. **18** As-Doped $Hg_{0.74}Cd_{0.26}Te$

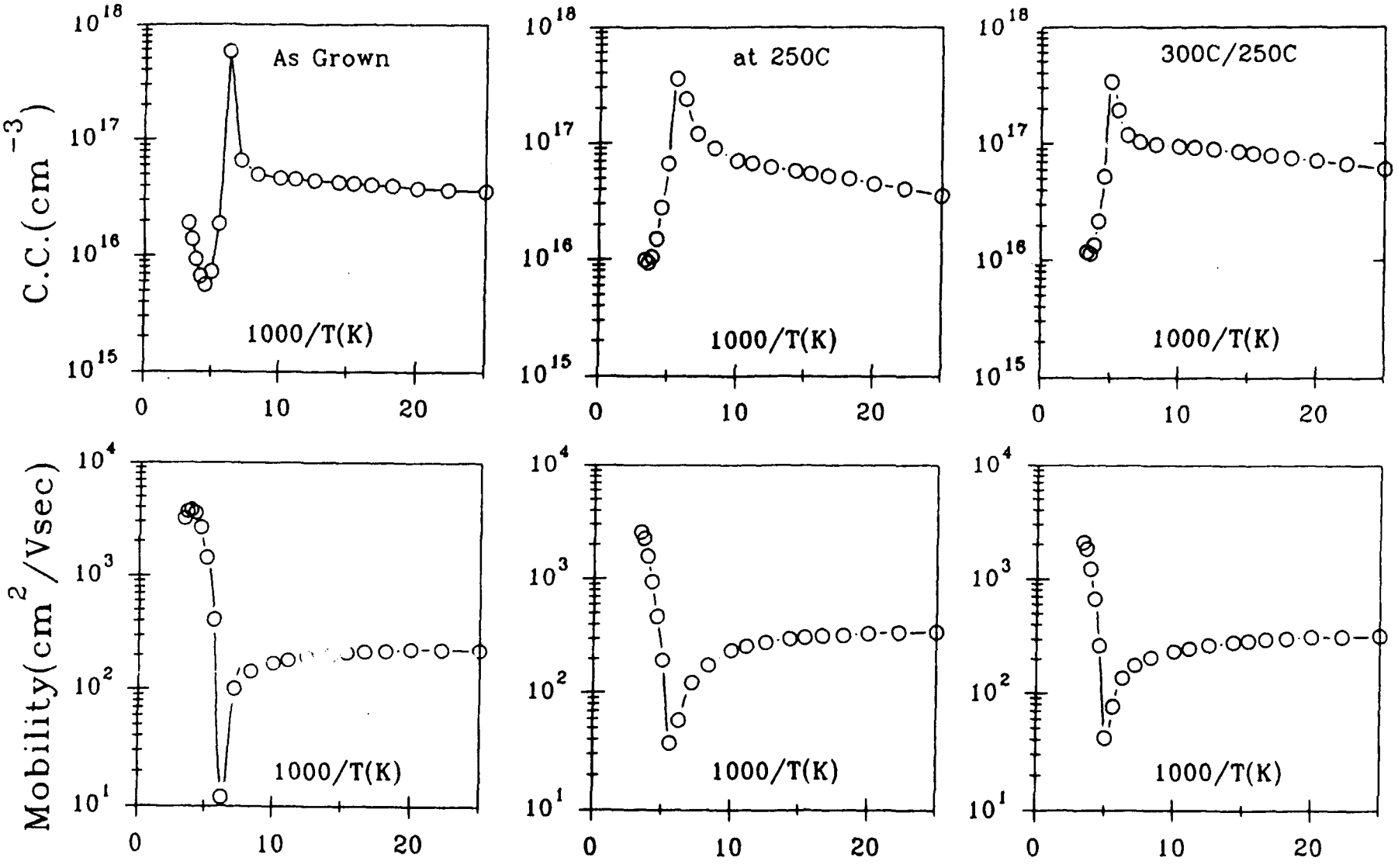

In summary 8 layers i.e. 33% of the As-delta doped epilayers show p-type character related to As in the as-grown state and/or after anneal at 250C. This is extremely encouraging and demonstrate that our approach is correct. These preliminary results might represent the solution expected regarding in-situ p-type doping of the MBE grown HgCdTe.

However the control of planar doping is not straightforward. The As doping profile is very critical in order to control the p-type behavior. EPIR has not been able, so far, to determine precisely which parameters induce with certainty the p-type character. In order to achieve such a control it will require a thorough investigation regarding growth temperature, delta doping spacing As flux control, As nature, i.e. As_4 vs As_2 and parameters of the growth interruption. **This represents a large research program going farther beyond the scope of EPIR's current project.**

Therefore at the very end of Year III we have worked on regular As-doped structures with the aim of achieving, after anneal, suitable heterostructures for IR detectors. However due EPIR's time consuming involement in As-delta doped layers we did not have enough time to carry out extensive investigations.

VII HETEROSTRUCTURES

Table VII displays n-on-n and p-on-n heterostructures grown mostly during the third year of this program. During Year II we have grown a 10-15 μm In-doped HgCdTe (x=0.22) grown on a (211)B substrate covered by a 1-2 μm HgCdTe undoped (x=0.33) itself passivated by a CdTe layer (heterostructures II-I of program goals). Such a structure is versatile since it can be the basis of n/p diodes (p-type anneal, followed by Hg diffusion or implantation) or p/n diodes (n-type anneal followed by As implantation). The first structure grown exhibits DCRC FWHM of 35 arcsec for x=0.22 layer and 40 arcsec for the top layer.

During Year III we have grown 21 heterostructures whose configurations are n-on-n (0.30 - 0.225) and p-on-n (0.30 - 0.225). In n-on-n heterostructures In has been incorporated in the base layer as well as in the cap layer. In p-on-n heterostructures In has been incorporated in the base layer

where as As has been evaporated during the growth of the cap layer (x=0.30). Arsenic introduced using this procedure is electrically activated after anneal at 436C/10 min followed by 250C/20 hrs anneal. During the growth of an heterostructure the change in the lattice parameter can induce dislocations. EPIR has worked out this problem. FWHM as low as 19 arcsec and EPD's in the low 10^5 cm^{-3} range have been measured. However more time was needed to achieve low EPD's on a regular basis.

VIII COLLABORATIONS

By the end of this program EPIR has reached a level of control in the production of high quality MBE grown HgCdTe layers allowing fruitful collaborations to take place.

Samples #145 and heterostructure 147 have been sent at the end of 1993 to Dr. Shin (Rockwell) who has performed the high temperature anneal on both of them. Dr. Shin prior to that had pocket implanted Arsenic for planar structure in sample 145. Dr. Shin then has returned the samples to EPIR without having device processed them for lack of ressources.

A collaboration has also began with Dr. Vyadanath from Aerojet. Once again due to restrictions in the Company, unfortunatly it has not been possible to establish the relation that EPIR was looking for.

IX MANUFACTURING PROCEDURES

During these three years EPIR has establish manufacturing procedures regarding the growth by MBE of In-doped HgCdTe (x=0.22) on (211)B CdZnTe substrates.

Standard deviation σ of 1.25% has been achieved on a total of 122 layers presenting an average composition $\bar{x}$=0.2236. A standard deviation σ of 0.59% and a yield of 80% have been obtained on the last 20 layers ($\bar{x}$=0.2204) grown in the program.

Composition uniformity σ_x of less than 5×10^{-4} accross a 2×2 cm^2 wafer and along the growth axis (thickness 11μm) have been measured. Thickness uniformity $\Delta d/d < 2.5\times10^{-3}$ accross a 2×2 cm^2 wafer has also been measured. These results are routinely obtained at EPIR whose standard MBE procedures are carried out with a rotating substrate.

EPD in the low 10^5 cm^{-2}, carrier concentration $N_d - N_a$ of less than 3×10^{15} cm^{-3}, electron mobility larger than 1×10^5 $cm^2v^{-1}s^{-1}$ and minority carrier lifetime larger than 0.5μs at 80K are characteristics routinely achieved at EPIR at the end of this program.

These characteristics are least as good if not better than those previously reported about LWIR HgCdTe material grown on the production line at SBRC(1) and therefore attest thatMBE grown HgCdTe produced at EPIR is a product suitable for IR photodiodes.

The manufacturing procedures have been extensively studied at EPIR and applied to the following parameters:

1. MBE system - maintenance, cleaning, regeneration of the cryo pumps, effusion cell out gassing.
2. Substrate screening and chemical cleaning.
3. Substrate introduction in the MBE system.
4. Substrate thermal cleaning.
5. Set up of effusion for growth.
6. HgCdTe growth calibration.
7. HgCdTe growth initiation - Precise control of substrate surface temperature and Hg flux - RHEED pattern monitoring.

8. HgCdTe growth - Pyrometer monitoring.

9. Dismounting, Gallium removal, block cleaning and sample storage.

10. Characterization of HgCdTe epilayer.

X SUMMARY

The summary of the achievements is presented at the begining of this final technical report. It illustrates that EPIR during this program has accomplished more than the targeted goals.

EPIR has indeed established manufacturing procedures to grow on a routine basis HgCdTe single layers suitable for LWIR photodiode fabrication. EPIR has been the first to report on impurity contamination from CdZnTe substrates. EPIR has also, for the very first time, proposed and implemented a new approach in terms of As doping i.e. the delta doping. The complexity of the approach has prevented EPIR to grow p-on-n heterostructures based on it. However the results are extremely encouraging since 33% of the 24 layers grown exhibit a p-type conduction due to As which does not require anneal above 250C. The delta doping approach thus preserves composition and doping profiles. EPIR has also actively tried to collaborate with other industries. For reftenchment in defense related programs long term relation could not have been, upto now, established.

XI REFERENCES

1. T. Tung, L.V. DeArmond, R.F. Herald, P.E. Herning, M.H. Kalisher, D.A. Olson, R.F. Risser, A.P. Stevens, and S.J. Tighe.
   SPIE, Vol. 1735, 109(1992)

2. S.M. Johnson, D.R. Ringer, J.P. Rosebeck, J.M. Peterson, S.M. Taylor, and M.E. Boyd
   J.Vac. Sci. Technol. B10, 1499(1992)

3. R.S. List. J. Electr. Mater. 22, 1017(1993)

4. M. Boukerche, P.S. Wijewarnasuriya, S. Sivananthan, I.K. Sou, Y.J. Kim, K.K. Mahavadi, and J.P. Faurie. J. Vac. Sci. Technol. A6, 2830(1988)

5. S. Sivananthan, X. Chu, J. Reno, and J.P. Faurie. J. Appl. Phys. 60, 1359(1986)

6. J.P. Faurie, R. Sporken, S. Sivananthan, and M.D. Lange. J. Cryst. Growth, 111,698(1991)

7. D.L. Polla and C.E. Jones. J. Appl. Phys. 52, 5118(1981)

8. M.E. de Souza, M. Boukerche, and J.P. Faurie. J. Appl. Phys. 68,5195(1990)

9. M.A. Kinch, M.J. Brau, and A. Simmons. J. Appl. Phys. 44, 1649(1973)

10. M.C. Chen and L. Colombo. J. Appl. Phys. 72, 4261(1992)

11. M.Y. Pines and O.M. Stafsudd. Infrared Phys. 20, 73(1980)

12. J.S. Blakemore. Semiconductor Statistics (Pergaman, New York, 1962)

13. R.G. Pratt, H. Hewett, P. Capper, C.L. Jones, and M.J. Quelch
    J. Appl. Phys. 54, 5152(1983)

14. P.R. Norton, Opt. Eng. 30, 1649(1991)

XII PROGRAM RELATED PUBLICATIONS

Papers

1. *Carrier recombination in indium-doped HgCdTe(211)B epitaxial layers grown by molecular beam epitaxy.*
   P.S. Wijewarnasuriya, M. Lange, S. Sivananthan and J.P. Faurie.
   J. Appl. Phys. 75,1005 (1994).

2. *Current status of the growth of HgCdTe by molecular beam epitaxy on(211)B CdZnTe substrates.*
   J.P. Faurie, S. Sivananthan, and P.S. Wijewarnasuriya.
   SPIE Vol. 1735, Infrared Detectors 1992.

3. *Minority carrier lifetime in indium-doped HgCdTe(211)B epitaxial layers grown by molecular beam epitaxy.*
   P.S. Wijewarnasuriya, M. Lange, S. Sivananthan and J.P. Faurie.
   Submitted for publication in Journal of Electronic Materials(in press).

4. *Arsenic-planar-doped p-type HgCdTe grown by MBE.*
   S. Sivananthan, J.P. Faurie, and P.S. Wijewarnasuriya.
   to be submitted.

Conferences and Professional Meetings

1. *Minority carrier lifetime in indium-doped HgCdTe(211)B epitaxial layers grown by molecular beam epitaxy.*
   P.S. Wijewarnasuriya, M. Lange, S. Sivananthan, and J.P. Faurie.
   The 1993 U.S. workshop on the Physics and Chemistry of Mercury Cadmium Telluride - Seattle, Washington(1993).

2. *Arsenic-planar-doped p-type HgCdTe grown by MBE.*

   S. Sivananthan, J.P. Faurie, and P.S. Wijewarnasuriya.

   The 1993 U.S. workshop on the Physics and Chemistry of Mercury Cadmium Telluride - Seattle, Washington(1993).

3. *Defect model for Arsenic-doped HgCdTe grown by MBE.*

   H.R. Vydyanath, L.S. Lichtmann, S.Sivananthan, P.S. Wijewarnasuriya, and J.P. Faurie.

   The 1993 U.S. workshop on the Physics and Chemistry of Mercury Cadmium Telluride - Seattle, Washington(1993).

4. *Current status of the growth of HgCdTe by molecular beam epitaxy on (211)B CdZnTe substrates.*

   J.P. Faurie, S. Sivananthan, and P.S. Wijewarnasuriya.

   SPIE conference, San Diego, California(July 1992).